



A review of multi-scale modelling, assessment, and improvement methods of the urban thermal and wind environment



Sihong Du ^{a,b}, Xinkai Zhang ^{a,b}, Xing Jin ^c, Xin Zhou ^c, Xing Shi ^{a,b,*}

^a College of Architecture and Urban Planning, Tongji University, Shanghai, 200092, China

^b Key Laboratory of Ecology and Energy-saving Study of Dense Habitat (Tongji University), Ministry of Education, Shanghai, 200092, China

^c School of Architecture, Southeast University, Nanjing, 210096, China

ARTICLE INFO

Keywords:

Urban thermal and wind environment
Simulation models and guidelines
Assessment indices and methods
Improvement strategies
Multi-scale

ABSTRACT

The urban thermal and wind environment (UTWE) has become a major concern in urban planning design. Consideration of the UTWE involves steps of modelling, assessment, and improvement on multiple scales. However, the method specifications of each step on different scales are unclear, and a comprehensive review of relevant studies is thus required. On this basis, the modelling, assessment, and improvement methods of the UTWE are comprehensively reviewed according to their applicable scales. The review indicates that the scale is systematically considered by studies of the UTWE modelling and improvement, but not by studies of UTWE assessment. On the meso-scale, the UTWE of plot units are usually evaluated in isolation and the interactions among them are neglected. Studies of the UTWE improvement cover urban morphology, urban green and blue infrastructure, and urban materials, but some of their conclusions contradict each other. Current UTWE assessments cannot directly guide the selection of proper improvement strategies. In the future, studies of the UTWE improvement may be based on urban typologies such as the Local Climate Zone, and the data-driven approaches provide an opportunity to link the results of UTWE assessment and the corresponding improvement strategies.

1. Introduction

1.1. Background

The world urbanization level has been rising with population increases and economic development. According to the United Nations, 68% of the world's population will live in cities by 2025 [1]. The urban environment has a significant impact on the physical health and daily life of people and the sustainability of the society. As essential components of the urban environment, the urban thermal environment and wind environment are closely inter-related and therefore are often considered simultaneously in urban design and other domains. The deterioration of the urban thermal and wind environment (UTWE) may exacerbate urban heat islands (UHIs) and air pollution problems [2–4], increase the energy consumption for indoor cooling and mechanical ventilation [5], and cause heat-related illness and even death [6,7].

The urban form can affect the UTWE in multiple ways. In urban areas, reduced vegetation and increased artificial pavements and

substrates lead to more solar radiation absorption, less evaporation, and less latent heat dissipation. Clustered buildings can exacerbate the thermal environment by impeding heat dissipation by longwave radiation and natural ventilation [8]. Many urban geometrical characteristics are found to significantly affect the UTWE, such as building density, building height, sky view factor, surface roughness length, and frontal area density [9–17]. Meanwhile, the increase of green cover ratio and green area ratio can lower the air temperature by providing shading and evaporation [10–14].

Consideration of the UTWE has become a major component of urban planning design, i.e., the UTWE-considered urban planning design. Many examples can be found in the literature. Ren et al. analysed the existing topography, land use, UHIs, natural landscape, and prevailing wind direction of Kaohsiung, Taiwan, and proposed several improvement strategies for urban heat mitigation, urban ventilation, and urban greening [18]. In Chengdu, China, the potential urban wind dynamics were classified based on the surface roughness and sky view factor, and several wind corridors were planned according to the classified potential

* Corresponding author. College of Architecture and Urban Planning, Tongji University, 1239 Siping Road, Shanghai, China.

E-mail addresses: sh_du@tongji.edu.cn (S. Du), zhangxinkai@tongji.edu.cn (X. Zhang), jxining@163.com (X. Jin), 101012014@seu.edu.cn (X. Zhou), 20101@tongji.edu.cn (X. Shi).

wind dynamics [17]. Based on the numerical simulation, Blocken et al. evaluated the improvement on the wind comfort and wind safety for a renovation scenario of an existing campus [19]. Based on the simulation of ENVI-met, Heris et al. compared the mitigation effect of different design scenarios on the UHI to pick out the most effective one [20].

The general workflow for the UTWE-considered urban planning design should consist of three steps, namely modelling, assessment, and improvement, as shown in Fig. 1. The objective of the modelling step is to acquire the most important information of the UTWE for the urban area considered. The information includes the air temperature, wind velocity, relative humidity, and mean radiation temperature. A variety of modelling techniques and tools is available for this step that will be reviewed in Section 2. Based on the acquired information, the assessment step involves evaluating the quality of the UTWE using certain indices and criteria which are covered in Section 3. The last step of the workflow is the improvement of the UTWE. Systematic and proper strategies are needed to mitigate problematic issues and improve the overall quality of the UTWE. Section 4 is dedicated to discussing these improvement strategies.

The UTWE involves factors on multiple scales, such as the topography and climate features on large scales [3,9,21,22], and spatial geometric morphology on small scales [12,23]. The characteristics of urban form on different scales are determined by different elements [24]. Therefore, a multi-scale perspective is needed in research on the UTWE [23]. For the study of UTWE modelling, the horizontal extent was defined as less than 2 km for the micro-scale, and 2–2000 km for the meso-scale, and the meso-scale can be further divided into meso- α , meso- β and meso- γ , of which the horizontal extent was defined as 200–2000 km, 20–200 km, and 2–20 km, respectively [25]. Multiple computational domains are usually nested to involve climate phenomena on different scales [26]. From a meteorological point of view, the UTWE can be classified as meso-scale, local scale, and micro-scale, generally corresponding to the urban/region scale, district/neighbourhood scale, and block/street scale in urban morphology [17,27,28]. Wong et al. stated that the meso-scale ranges from a few to several hundred kilometres, the local scale from a few hundred meters to a few kilometres, and the micro-scale from a few meters to several hundred meters [27]. The relationship between the working scales of urban planning design and meteorological studies was mapped by Ren et al. [17].

The determinant factors for the UTWE on different scales are not the same. On the meso-scale, the spatial UTWE patterns are not only affected by urban form, but also significantly relate to topographic factors, such as the altitude, sea-land breeze, and mountain-valley breeze [9,17,21,22]. However, the effect of topographical variation is relatively limited and less influential on the local and micro scales. Instead, the effect of urban form, including the structure of street networks and the morphology of street canyons and building clusters, becomes more significant [12,29,30]. In addition, the correlation between the UTWE and the same morphological factors can also vary with the scale. The contributions of the urban morphological factors to the air temperature and land surface temperature have been found to be largely scale-dependent [31,32]. Local UTWEs were found to have different dependences on their surrounding urban forms at different scales [13,15,16,33]. Fig. 2 illustrates the three scales of the UTWE and their

corresponding scales in urban morphology.

1.2. Previous reviews

Some previous reviews are relevant to the modelling, assessment, and improvement methods of the UTWE. Most of them only focused on a single aspect, such as modelling methods of the UTWE [34–36], outdoor thermal comfort assessment [37] and wind comfort criteria [38], the assessment indices of urban ventilation [39], and the effects of urban morphology, vegetation, and materials on the UTWE [30,40–43]. Several reviews simultaneously examined the UTWE assessment parameters and modelling tools, indicating that an integrated modelling interface is needed because the UTWE assessment involves multiple parameters [44,45]. Although such reviews provide insights into some specific aspects of the modelling, assessment, or improvement methods of the UTWE, two limitations may also be noted.

First, a systematic review of the modelling, assessment, and improvement methods of the UTWE is needed, because the three steps constitute an integrated workflow of the UTWE-considered urban planning design. This would provide a broader insight into the integrated workflow for urban planners and engineers. Furthermore, the three steps are closely connected to each other; each step should provide sufficient information for the next. Therefore, a systematic review would be helpful to capture the limitations of current methods based on the requirements of each step. Some limitations of current methods may be detected from reviews on a single step, such as the problems to be solved for computational fluid dynamics (CFD) modelling [46], the consideration of dynamic UTWE for outdoor thermal comfort modelling [37], and the feasibility of ventilation indices for complex urban morphology [39]. However, a more elaborate and comprehensive understanding about the limitations of current methods could be achieved from the systematic review.

Second, a multi-scale perspective should be introduced for the study of the UTWE. The differences in scales influence not only the determinant factors of the UTWE, but also the computational and design cost in the realistic design process. Therefore, the scale can influence the methods of modelling, assessment, and improvement of the UTWE both theoretically and empirically. Although the multi-scale approach has been considered by some UTWE studies [23,27,34,47], most reviews still focus on a single scale or neglect to analyse the applicable scales of the reviewed methods. Therefore, a multi-scale review would provide in-depth understanding of the specific requirements of different scales in terms of the modelling, assessment, and improvement of the UTWE.

1.3. Objective and scope of this review

Considering the background and research gaps discussed above, a systematic review of the modelling, assessment, and improvement methods of the UTWE on multiple scales was conducted, including common models and tools, assessment indices and assessment cases, and improvement strategies of the UTWE. The objective of this review can be summarized as follows.

- 1) Investigating whether the urban scale is properly concerned in studies of the modelling, assessment, and improvement of the UTWE,

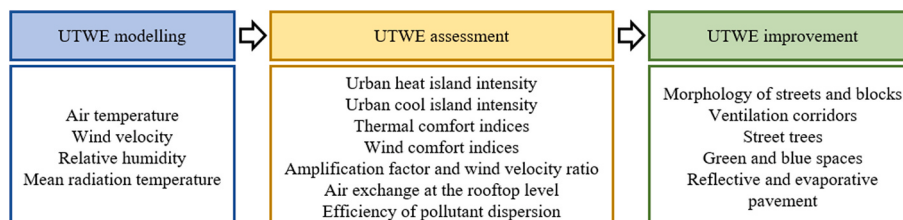


Fig. 1. Steps of considering the UTWE in urban planning design and examples to consider at each step.

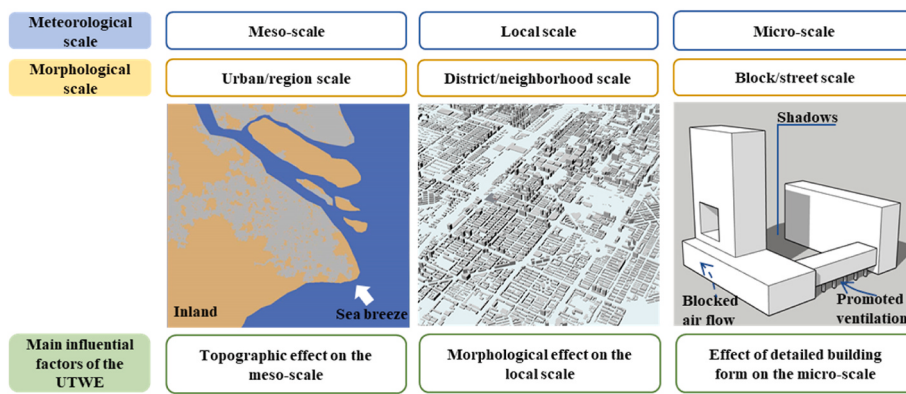


Fig. 2. Classification of the urban scale.

- and whether the current methods of each step are suitable for different scales.
- 2) Investigating whether the current methods of the modelling, assessment, and improvement of the UTWE meet the specific needs of each other, considering the close connection among the three steps in urban planning design.
 - 3) Providing insights into the challenges and opportunities of future studies of the UTWE, and references to consider the UTWE in urban planning design.

From the perspective of urban planning design, literature about the following topics is the core literature in this review.

- 1) Literature about UTWE modelling, including the models and corresponding modelling tools, and the guidelines and validation studies of the modelling tools. The modelling tools mainly include those which have been commonly used in the assessment and improvement studies of the UTWE.
- 2) Literature about the assessment of the UTWE on different scales, including the assessment indices and criteria, and case studies of the UTWE assessment.
- 3) Literature about the design strategies to improve the UTWE, including strategies to mitigate the urban heat island, and improve outdoor thermal comfort and urban ventilation.
- 4) Literature about the effect of urban forms on the UTWE because it is directly associated with the assessment and improvement of the UTWE.

Articles about the topics above were collected from the Web of Science Core Collection by searching the following keywords.

- Keywords of the UTWE modelling: combinations of “urban microclimate or thermal/wind environment” and “simulation/model/validation/practice/guideline”.
- Keywords of the UTWE assessment: combinations of “assessment/evaluation/criteria/indices” and “urban thermal/wind environment, outdoor thermal/wind comfort or urban ventilation”.
- Keywords of the UTWE improvement: “urban heat island mitigation”, “improve/enhance outdoor thermal/wind comfort/environment”, “urban ventilation corridors or air path”, “cooling effect of urban green/blue spaces/infrastructures”, “urban cool island”, and “effect/impact of urban form/morphology/design on microclimate or thermal/wind environment”.

The collected articles were filtered according to the principles above. On this basis, other relevant literature cited by these articles was further supplemented. Finally, a total of 200 articles were selected as core literature, which was all written in English and published during 1963 and 2021.

1.4. Structures of this review

The literature review is organized as follows. In Section 2, a variety of commonly used models and tools of the UTWE are reviewed, together with their practice guidelines, validation and practice cases. In Section 3, assessment indices and criteria of the UTWE are introduced and compared. Case studies are further reviewed to investigate the common treatments of the dynamic UTWE in actual urban spaces on different scales. In Section 4, improvement strategies of the UTWE are reviewed according to their applicable scale, including urban morphology, urban green and blue infrastructures, and urban materials. In Section 5, methodological differences of the modelling, assessment, and improvement methods of the UTWE among different scales are discussed. Some limitations of the relevant methods are highlighted and corresponding insights are proposed for future studies.

2. Modelling of the UTWE

Although field measurement and thermal remote sensing can be used to obtain climatic parameters for existing urban areas, theoretical modelling, i.e., simulation, remains the most effective and efficient approach to study the UTWE in an urban planning design project. This section reviews the models and guidelines for modelling the UTWE on the micro-scale, local scale, and meso-scale.

2.1. Models and tools for different scales

Currently, the dynamical numerical models are commonly used to simultaneously simulate the UTWE on different scales. Such models include the CFD models for the micro/local scale and the meso-scale models which further resolve large-scale interactions under the Planetary Boundary Layer (PBL) [34]. Meanwhile, the urban canopy models (UCMs) based on the energy conservation law are usually integrated with the meso-scale models to improve the ability to simulate surface or near-surface air temperatures in the urban areas and their surroundings [48]. The features and relevant tools of these models are introduced in terms of their applicable scales in this section.

2.1.1. Models and tools for the micro-scale and local scale

On the micro-scale and local scale, studies usually require UTWE fields with high resolution in the urban canopy layer. Therefore, the CFD models have been widely used because they can simulate with high-resolution and be coupled with multiple physical models. The UTWE can be simulated by CFD models using actual geometrical models of the considered urban areas [34]. The transport equations are solved by finite volume methods with a resolution of several meters [49]. Coupled simulations of convection, radiation and conduction are further performed for the modelling of the thermal environment [50,51], and the humidity and pollution fields can also be coupled if necessary [42].

Multi-physics coupling is necessary to simulate the thermal environment of a realistic world with soil, water bodies, and vegetation. For example, coupling with models of water bodies can simulate the cooling effect of urban blue spaces by calculating evaporation, transmission and absorption of shortwave radiation inside the water, and the effect of turbulent motion on air-water energy exchange [52,53]. Coupling of the vegetation model and soil model can improve the accuracy to simulate the evaporation and transpiration of the vegetation by calculating the vegetation water supply, and the evaporative cooling of vegetation can be estimated by such methods [54,55].

Due to the features of CFD models, relevant commercial tools that can be used to simulate the high-resolution UTWE are widely available nowadays. Fluent, Phoenics, scSTREAM, OpenFOAM, and ENVI-met are frequently used and found in the literature. Detailed introductions to each software package are provided on their official websites [56–60]. ENVI-met has been increasingly used for simulating the UTWE on the micro-scale and local scale due to its features [35,36]. However, the choice of turbulence models of ENVI-met is less comprehensive than those of other universal CFD tools, and large eddy simulation (LES) models are not provided.

Despite the high resolution and simultaneous solution of multiple equations of the CFD models, enlarging the simulation scale can significantly increase the computational cost. Therefore, most simulations with CFD models are limited to an extent of $2 \times 2 \text{ km}^2$ [35]. To observe the accurate wind field and its interaction with the temperature field, some simulations of an extent of 10–30 km have also employed CFD models [21,61,62]. For the UTWE modelling on larger scales, meso-scale models and UCMs should be employed.

2.1.2. Models and tools for the meso-scale

The meso-scale models can be distinguished from CFD models in terms of the physical phenomena considered, spatial resolution, and urban morphology simplification. Large-scale interactions under the PBL are considered by meso-scale models [34]. Because of the coarse spatial resolution of the meso-scale models, details of the urban canopies are replaced with bulk urban parameters [34,63]. This treatment decreases the ability of meso-scale models to simulate the UTWE compared with CFD models [34,61].

UCMs are based on the energy conservation law within a control volume and consider the energy exchanges among surfaces and ambient air in the urban canopy [34]. In the UCMs, airflow is decoupled from the temperature field and defined as a particular input into the control volume [34,42]. Buildings within the control volume are simplified homogeneously by urban canopy parameters, rather than actual geometrical models [34,48]. By simplifying the urban canopy geometries to different degrees, three types of UCMs are developed, including the slab model, single-layer canopy model, and multi-layer canopy model [48]. Tools such as urban weather generators [64], building effect parameterization [65], and canopy interface models [66] have been proposed based on the UCMs.

To improve the accuracy of UTWE modelling on the meso-scale, UCMs and meso-scale models are usually coupled. An integrated modelling system, the weather research and forecasting (WRF) model, is commonly used for UTWE modelling on the meso-scale. To improve the ability to simulate the UTWE in complex urban areas, several PBL models, fine-scale CFD Reynolds-averaged Navier-Stokes and the LES models, UCMs, and a land data assimilation system were integrated [63]. A study showed that coupling the single-layer and multi-layer canopy model in the WRF provided more accurate predictions of the air temperature than coupling the bulk scheme of slab model, and the multi-layer canopy model performed the best for simulating the UTWE in urban areas with sophisticated structures [48]. The urban canopy parameters for the WRF modelling can be achieved from the World Urban Database and Access Portal Tool (WUDAPT) [67] and National Urban Database and Access Portal Tool [68], or derived from open-source maps, satellite remote sensing, and global digital elevation

models [69–71].

2.1.3. Coupling of multi-scale simulation

It is noted that initial boundary conditions of the UTWE modelling are set constant or simplified by approximate functions such as the power law of vertical wind profile, which is different from the conditions in realistic urban areas [46]. Therefore, some methods of multi-scale modelling of the UTWE are proposed to obtain more accurate initial boundary conditions for a targeted area from simulation of extended areas. From the perspective of numerical simulation, the multi-scale simulations include multi-scale systems and multi-scale processes, and the former simulates with the same governing equations on each scale but the latter involves different governing equations and suitable numerical methods on each scale [72,73].

For the multi-scale system, Tang and Joshi proposed a multi-grid embedded multi-scale approach [74]. Cui et al. further employed this method to simulate the indoor airflow and pollutant transfer by CFD models considering the effect of neighbourhood scale and street scale, which extracted and interpolated UTWE parameters at the outlet of the larger domain as the boundary conditions for the smaller domain [75].

For the multi-scale process, the method is to solve the process on each scale by different numerical methods and exchange the information at the interfaces between each scale [73]. To involve the effect of meso-scale phenomena for the modelling of UTWE on micro-scale or local scale, a common method is to integrate meso-scale models and CFD models. Obtaining meso-scale wind flow from WRF, the wind flow of a coarse grid can be further downscaled by CFD models by assigning wind velocity boundary conditions at the inlet faces of the CFD domain according to WRF outputs [76,77]. Wong et al. integrated WRF and CFD models to achieve accurate boundary conditions for micro-scale modelling by a nested-down approach that continuously forced meso-scale weather at lateral boundaries of the CFD model domains [27]. By coupling CFD models and building energy models such as EnergyPlus, the effects of the surrounding thermal and wind environment can be involved by the simulation of building energy consumption [27,78–80].

2.2. Guidelines for modelling tools practice

Besides the features of the UTWE models, the modelling accuracy is also determined by the practice of users, such as the settings of input parameters, urban geometrical models, and computational domains. In this section, guidelines for the CFD models are reviewed for the UTWE modelling on the micro-scale and local scale, and guidelines for the WRF model and its integration with the UCMs are reviewed for the UTWE modelling on the meso-scale.

2.2.1. Guidelines of UTWE modelling on the micro-scale and local scale

For CFD modelling of the urban wind environment, suggestions can be referenced from the guidelines of two organizations, COST [81] and AIJ [82], including the settings of the computational domain, grid discretization, boundary condition, convergence solution, and turbulence models. However, other recommendations on urban geometry modelling are supplemented to address the complexity of realistic urban morphology. An et al. provided advice about the treatment of topography to improve the accuracy of wind-environment modelling [83]. Tong et al. investigated the definition of influential urban regions to provide accurate boundary conditions for targeted buildings [84].

For CFD modelling of the urban thermal environment, settings in regard to the radiation, initial thermal condition, and transient simulation should be further concerned. However, formal guidelines are not currently available, and references were summarized from some practices of modelling cases and model validation studies. The setting of grid resolution can influence modelling accuracy of the thermal environment by determining shadings [85]. A horizontal resolution of 2 m was recommended by some studies to achieve reliable results and acceptable

modelling efficiency [85,86]. Temperatures at the model inflow boundary were reported to be significantly higher than those in the inner areas because of the excessive solar radiation in the un-shaded nesting area [32,87]. This phenomenon was found to be inconspicuous after the first 200 m in the windward direction [32]. Deng et al. extended the geometric models to a block scale around the considered urban area to minimize boundary effects [88]. At the beginning of a simulation, the surface temperature and air temperature in the computational domain are set uniform, which is different from realistic urban thermal conditions. Therefore, the simulation is suggested to be started at sunrise or during the night when the temperature differences are relatively limited so that the calculation can follow the atmospheric process [85,86]. Moreover, an initialization time of 24–48 h is needed to reproduce more realistic initial thermal conditions for the subsequent simulation period [86,88]. Only considering the accuracy of air temperature, Zhang et al. found that increasing the initialization time from 4 h to 7 h only improved the model performance slightly [89]. Because of the involvement of transient simulation, settings of the update intervals and time steps should be considered, which can be referenced from the recommendations of ENVI-met [90,91].

It is noted that the CFD guidelines above aim to precisely simulate the UTWE. Applying such guidelines on the local scale would entail extensive computational load. When assessing the UTWE on the local scale, spaces of interest are usually the streets and public spaces (see Section 3.3). From this point of view, precisely simulating the UTWE for every corner and alley may also not be necessary. Further studies may investigate how to simulate the UTWE on the local scale with simplified geometric models and relatively coarse resolution to achieve satisfying results for the main streets and public spaces. A relevant study has been conducted by Ricci et al. which investigated the influence of geometrical simplification on simulated mean vertical wind-velocity profiles [92].

2.2.2. Guidelines of UTWE modelling on the meso-scale

Settings of the WRF include physics schemes, computational domain, model initialization, and urban canopy parameters (UCPs) [48]. The available physics schemes can refer to the technique report of the WRF [93]. The computational domain of the WRF can consist of three or four nested domains, with the central domain covering an urban scale and the outmost domain covering several hundred kilometres. The horizontal grid resolutions are usually set at several hundreds of meters to 1 km for the central domain and a few tens of kilometres for the outmost domain [47,48,94,95]. Initialization time is also needed for the WRF, and the output values of the first 24 h are usually discarded [47,95].

The inputting of UCPs is an important process influencing the modelling performance of the WRF. Three approaches are available to specify the UCPs for the grids, namely urban land-use maps and urban-parameter tables (tabulated-UCPs), gridded high-resolution UCPs data sets (gridded-UCPs), and a mixture of these [63]. Zhang et al. found that gridded-UCPs contributed to more precise results in dense urban areas and heterogenous spaces [95]. When the actual UCPs are not available, the datasets of WUDAPT can be an alternative choice. However, the use of UCPs from WUDAPT may decrease the modelling accuracy versus UCPs derived from actual urban morphology [94,96].

3. Assessment methods of the UTWE

To assess the UTWE, three questions need to be answered: (1) what indices can be used? (2) where and when should these indices be evaluated? and (3) how should we assess the temporally-spatially dynamic UTWE based on the assessment indices? The assessment indices reflect certain aspects of the UTWE, such as urban heat island effects, outdoor thermal/wind comfort, and natural ventilation. Spaces and periods of interest are usually extracted for assessment, and the UTWE can be evaluated by the spatial and temporal patterns of the assessment indices. Further, statistical values such as the maximum, minimum, or average of particular assessment indices per unit space and time are usually

calculated to evaluate the temporally-spatially dynamic UTWE. Currently, a systematic assessment method covering these issues has not been proposed. Some case studies involving UTWE assessment on different scales are thus reviewed in this section. The general assessment procedures are illustrated in Fig. 3.

3.1. Indices to assess the urban thermal environment

Assessment of the urban thermal environment in urban planning design aims to measure the impact of urban forms on the air temperature and thermal comfort of human beings. Therefore, indices related to the urban heat island and urban cool island (UCI) are frequently used, and some indices are developed to measure outdoor thermal comfort. The relevant indices are reviewed in this section.

3.1.1. Air temperature, urban heat island intensity and cool island intensity

The air temperature, the urban heat island intensity (UHII) and urban cool island intensity (UCII) are directly associated with the urban thermal environment. The air temperature at the pedestrian level is often acquired for the assessment of the urban thermal environment. Due to the temporal variation of the air temperature, its daily range, daily maximum, daily minimum, daily average, and average during daytime and night are usually used to evaluate the impact of urban form on the thermal environment or compare the thermal performance of different urban scenarios [12–15,87,97–99].

Compared with the air temperature, the UHII and UCII can be more effective for measuring the heating and cooling effects of the urban form. The UHII and UCII refer to the temperature difference between the urban area and the surrounding rural area. The air temperatures recorded at the meteorological stations in suburban areas are commonly used as the baseline temperature for the UHII/UCII. To provide a consistent baseline temperature for studies from different cities, Stewart and Oke proposed a Local Climate Zone (LCZ) scheme to classify urban areas into 10 built types and 7 land cover types [100]. In this way, the average air temperature of low-plant areas (LCZ D) can be used as the baseline temperature for the UHII/UCII [97,101].

Since the UHII/UCII at any certain time or their average values over a period cannot fully describe heating and cooling effects, Yang et al. proposed UHI/UCI degree hours to measure the duration of the UHI/UCI [102]. Meanwhile, considering that the UHI/UCI is generated because of the different rates of warming and cooling between urban areas and their surroundings, Yang et al. proposed hourly warming and hourly cooling rates to measure this effect of urban areas [101].

3.1.2. Outdoor thermal comfort

Besides indices associated with the air temperature, the assessment of the urban thermal environment also considers the thermal comfort of human beings, which is not only affected by the air temperature but is also related to other factors, such as relative humidity, wind speed, mean radiation temperature, metabolic rate, skin temperature, and the isolation value of clothing. Therefore, a variety of theoretical thermal comfort models have been developed to evaluate the thermal comfort level in urban spaces. They are developed based on the human thermal balance, which can be further divided into equivalent temperature models and thermal load models [37].

Thermal comfort indices calculated by the equivalent temperature models include the Physiologically Equivalent Temperature (PET) [103], the New Standard Effective Temperature (SET) [104], the Outdoor Effective Temperature (Out_SET) [105], and the Universal Thermal Climate Index (UTCI) [106]. These indices are generally defined as the equivalent air temperature of a standard environment which generates the same physiological responses. The major difference among these indices is the treatment of human heat transfer [37]. The PET, the SET, and the Out_SET are based on different two-node models [104,107] which consider the effects of skin temperature and core temperature on the human heat balance [108]. Nevertheless, the UTCI is based on

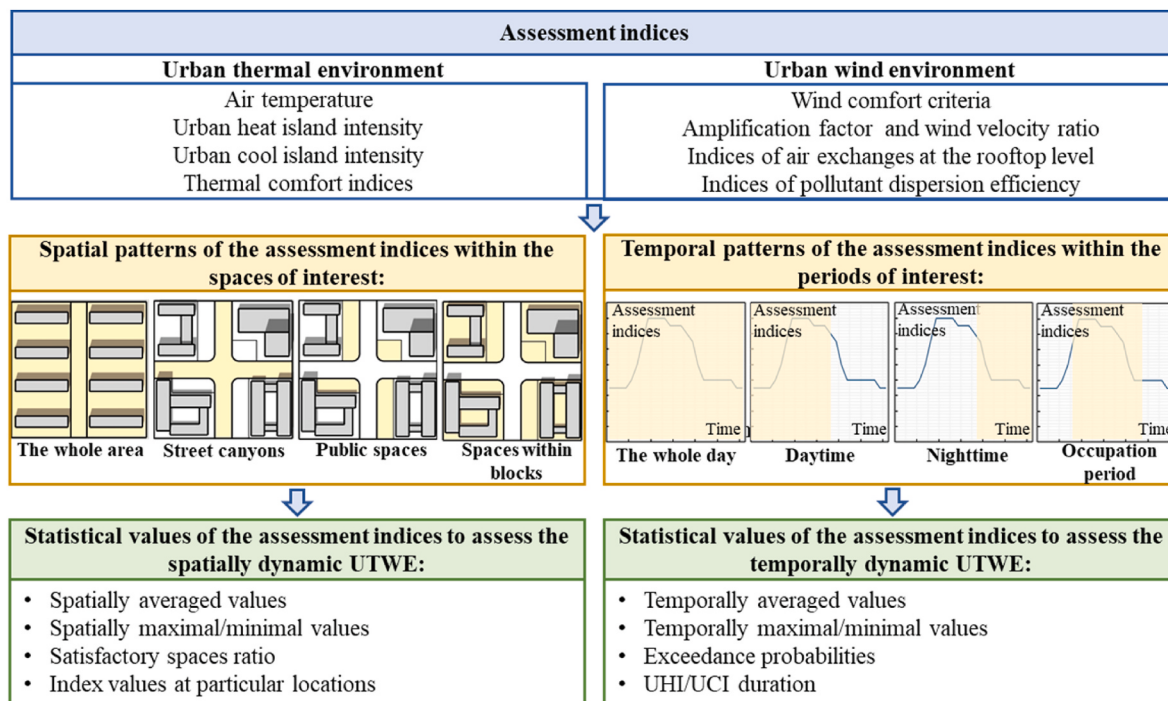


Fig. 3. General assessment procedure of the urban thermal and wind environment (UTWE).

Fiala's multi-node model, which considers the heat transfer among multiple segments within the body and further employs a self-adaptive clothing model [109]. It thus treats the human body in greater detail and better predicts both overall and local physiological responses than the two-node models [106].

Thermal comfort indices calculated by the thermal load models include the Predicted Mean Vote (PMV) [110], the COMfort Formula (COMFA) [111], and the Index of Thermal Stress (ITS) [112]. The PMV model, defined as the average thermal sensation vote of a group of people, was developed based on Fanger's heat balance model [110] and later adapted to outdoor conditions by adding shortwave and longwave radiation fluxes [113]. The COMFA model was first developed by Brown and Gillespie and was later revised as the COMFA + model to take the effect of urban forms on energy budget into consideration [114–116]. The ITS represents the ratio between the necessary sweat rate to maintain the thermal equilibrium and the cooling efficiency of the body [112]. It was later adapted for the urban thermal environment by Pearlmuter et al. [117]. Despite its use in urban areas, the PMV may tend to overestimate the out-thermal sensation according to several studies [118,119], and the validity of the COMFA and ITS models has not been sufficiently demonstrated [37].

Besides the intrinsic features influencing the predictive abilities of these indices, the context of regions also matters. Compared with other thermal comfort indices, the UTCI was suggested to be capable of predicting the thermal comfort under various climates, weather, and locations, and of being very sensitive to the changes in ambient stimuli [120]. However, a study in Shanghai, China, indicated that the COMFA is a more accurate model than the PET and the UTCI [121]. In an arid city, Mendoza, Argentina, the percentages of predictive ability of the PET, PMV, and COMFA were found to be lower than 25% [122]. When the operative temperature exceeded 34 °C, the relationships between mean thermal sensation and the thermal comfort indices such as the PET, SET, UTCI and PMV tended to become blurred [108]. Despite these limitations, Ruiz et al. stated that these indices are still capable of diagnosing the degree and frequency of thermal comfort for urban spaces in the stage of urban planning design [122].

3.2. Indices to assess the urban wind environment

Assessment of the urban wind environment involves more perspectives, including the wind comfort criteria, wind resistance, and ventilation efficiency. The wind resistance can be measured by amplification factor and wind velocity ratio. The ventilation efficiency can be measured by air exchange caused by turbulent fluctuations at the rooftop level and pollutant dispersion efficiency. The relevant indices are reviewed in this section.

3.2.1. Wind comfort criteria

According to a review of Koss et al., the outdoor wind comfort can be evaluated according to the gust wind speed (U_g) and mean wind speed (U_m), their thresholds, and the corresponding acceptable exceedance probability [38]. The commonly used wind comfort criteria are listed in Table 1. Koss et al. [38] stated that the gust wind speed was further defined as the equivalent steady wind speed by Hunt et al. [123] and the peak gust wind speed by Melbourne [124]. All of them can be expressed by Eq. (1), where U_g represents the gust wind speed, U_m the mean wind speed, g the gust factor, and σ_v is the standard deviation of the wind speed [38]. The value of g was defined as 3 for the equivalent steady wind speed [123], 3.5 for the peak gust wind speed [124], and 2.68 by Lawson and Penwarden [125]. Isyumov and Davenport [126], and Soligo et al. [127] used the mean wind speed to evaluate the wind comfort.

$$U_g = U_m + g \cdot \sigma_v \quad (1)$$

The comfort thresholds of the U_g and U_m were defined according to activity types [125,127], residence time [124,126], and dangerous conditions [124,127]. The acceptable exceedance probability refers to the allowable frequencies of the U_g and U_m exceeding the predefined thresholds within a certain duration of time [38]. Melbourne defined the thresholds of the peak gust wind speed as 10 m/s to 16 m/s for different activities, and the exceedance probability was limited to 0.002% [124]. This criterion was thus suggested as suitable for evaluating the strong wind condition [128]. In comparison, Soligo et al. defined the thresholds of the mean wind speed as 2.5 m/s to 5 m/s for different activities, and

Table 1
Wind comfort criteria.

Wind comfort criteria	Category	Threshold value	Exceedance probability
Isyumov and Davenport [126]: $U_g = U_m + 1.5\sigma_v$	Long	$U_m < 3.58$ m/s	1.5% 0.3%
		$U_m < 5.37$ m/s	
		$U_m < 5.37$ m/s	
		$U_m < 7.61$ m/s	
	Short	$U_m < 5.37$ m/s	1.5% 0.3%
		$U_m < 9.85$ m/s	
		$U_m < 12.53$ m/s	
		$U_g > 15.22$ m/s	0.02%
		$U_m < 2.5$ m/ s	20%
Soligo et al. [127]:	Sitting	$U_m < 3.9$ m/ s	20%
	Standing	$U_m < 5$ m/s	20%
	Walking	$U_m < 14.44$ m/s	0.1%
	Dangerous	$U_m < 13.85$ m/s	2%
	Covered area	$U_m < 3.35$ m/s	4%
	Standing area	$U_g < 5.7$ m/s	
		$U_m < 5.45$ m/s	4%
		$U_g < 9.3$ m/s	
		$U_m < 7.95$ m/s	4%
		$U_g < 13.6$ m/s	
Lawson and Penwarden [125]: $U_g = U_m + 2.68\sigma_v$	Unacceptable	$U_g < 23.7$ m/s	
	Walking area	All other cases	
	Uncomfortable	$U_g < 6$ m/s	10%
	Comfort and little effect on performance	$U_g < 9$ m/s	10%
	Most performance unaffected	$U_g < 15$ m/s	10%
	Control of walking	$U_g < 20$ m/s	10%
	Safety of walking	$U_m > 9$ m/s	1%
	Unacceptable	$U_g < 10$ m/s	0.002%
	Long exposure	$U_g < 13$ m/s	0.002%
	Short exposure	$U_g < 16$ m/s	0.002%
Melbourne [124]: $U_g = U_m + 3.5\sigma_v$	Walking	$U_g > 23$ m/s	0.002%
	Danger		

the exceedance probability as 20% [127]. This criterion is easily used by urban planners, and the exceedance probability is generally deemed reasonable because it agrees with local planning authorities based on their experience [128,129]. The criterion of Hunt was deemed to be concise but lacked a confidence survey [128].

It has been noted that these criteria only define the upper limit of the wind speed threshold. Du et al. defined the low wind threshold value of 1.5 m/s and the exceedance probability of 50% for the assessment of wind comfort in summer [128]. This suggestion was proposed based on human minimum noticeable wind speed [125] and the requirement to achieve a neutral thermal sensation under shaded conditions in summer [130].

3.2.2. Amplification factor and wind velocity ratio

The amplification factor (AF) and wind velocity ratio (WVR) can be used to measure the wind resistance of urban fabrics. Their equations are listed in Table 2. The definition of AF is the ratio of the local wind

Table 2
Equations of the amplification factor (AF) and wind velocity ratio (WVR).

Indices	Equation	Variable description
AF [131]	(2) $AF = \frac{U_L}{U_{R1}}$	U_L : local wind speed at building site U_{R1} : wind speed at rural meteorological site
WVR [132]	(3) $WVR = \frac{U_L}{U_{R2}}$	U_{R2} : wind speed at the top of the wind boundary layer which is not affected by the ground roughness

velocity at the pedestrian level to the wind velocity in rural areas at the same level, as shown in Eq. (2) [131]. The definition of WVR is the ratio of the local wind velocity at the pedestrian level to the wind velocity at the top of the wind boundary layer which is not affected by the ground roughness, as shown in Eq. (3) [132]. In comparison with the WVR, the AF value can more intuitively reflect the wind resistance effect of local urban fabrics. The urban fabrics show acceleration effects on local ventilation when the AF is larger than 1, and resistance effects on local ventilation when it is less than 1.

3.2.3. Air exchange at the rooftop level

The air exchange at the rooftop level caused by turbulence can effectively influence the pollutant removal in the urban canyons. Several indices have been derived to evaluate this process, including the air exchange velocity (U_e), the pollutant exchange velocity ($U_{e, pollutant}$), the roof air exchange rate (ACH_{roof}), the pollutant exchange rate (PCH), and the revised roof air exchange rate ($R-ACH_{roof}$). Equations for these indices are listed in Table 3. U_e is defined as the ratio of the momentum flux to the difference between the mass flux above and below the top of urban canopy, as shown in Eq. (4) [133]. U_c represents the spatially and temporally simplified in-canopy velocity, as shown in Eq. (5), where F_p is the pressure force acting on the building, C_D is the drag coefficient, ρ is the air density, and A_f is the building frontal area [133]. Based on the definition of U_e , the $U_{e, pollutant}$ between the in-canopy and the overlying atmosphere through the roof can be derived as Eq. (6) [134].

$$U_c = \sqrt{\frac{2F_p}{\rho C_D A_f}} \quad (5)$$

ACH_{roof} represents the rate of air exchange between the urban

Table 3
Indices of air exchange at the rooftop level.

Indices	Equation	Variable description
U_e [133]	(4) $U_e = \frac{\int_A (\bar{u}w + \bar{u}'w') dA}{A(U_{ref} - U_c)}$	$(\bar{u}w + \bar{u}'w')$: mean and turbulent contributions of the vertical momentum flux at roof level through the exchange surface A ; U_{ref} : free upstream velocity at the boundary; U_c : spatially and temporally simplified in-canopy velocity.
$U_{e, pollutant}$ [134]	(6) $U_{e, pollutant} = \frac{\int_A (\bar{c}w + \bar{c}'w') dA}{AC}$	\bar{c} : spatially-averaged pollutant concentration within the urban canopy; $(\bar{c}w + \bar{c}'w')$: mean and turbulent contributions of the pollutant flux at roof level through the exchange surface A .
ACH_{roof} [135]	(7) $ACH_{roof}(t) = \int_A w''(t) _{roof} dA$	$w''(t) _{roof}$: roof-level fluctuating vertical velocity along the roof area A across the street at time t .
PCH [39]	(8) $PCH(t) = \int_A w''(t) _{roof} \bar{c}(t) _{roof} dA$	$\bar{c}(t) _{roof}$: pollutant concentration in the street
$R-ACH_{roof}$ [136]	(9) $R-ACH_{roof}(t) = \frac{\int_{\Omega} w''_{+} d\Omega}{\int_{\Omega} d\Omega}$	Ω : RSL domain and subscript + denotes the upward flows only.

canopy and free atmosphere above, as defined by Eq. (7) [135]. The mean vertical velocity at roof level is neglected in this equation because the roof-level air exchange is largely governed by the turbulent component [39]. Based on the definition of ACH_{roof} , the PCH of the pollutants entering or exiting the urban canyon can be derived as Eq. (8) [39]. To use ACH_{roof} and PCH , the roof-level of urban canyons should be clearly defined, which is difficult for urban areas with non-uniform building heights. Meanwhile, street ventilation is mainly governed by the dynamics of the roughness sublayer (RSL), not those along the building-roof level [136]. Therefore, $R-ACH_{roof}$ was proposed for urban areas with various building heights, defined in Eq. (9) [136].

Estimating the air exchange at the roof-top level requires the use of wind tunnel experiments or LES models [135,136], because the fluctuating velocity cannot be solved by RANS k-e turbulence models. However, the two methods involve numerous financial costs or computational loads, and the LES models are not provided by some popular tools such as the ENVI-met. Therefore, Li et al. used the isotropic turbulence assumption ($u'' = v'' = w''$) to estimate ACH with RANS k-e turbulence models [137], whereby $w'' = 2/3k$ and Eq. (8) can be finally expressed by Eq. (10), where k denotes the turbulent kinetic energy at roof level [137]. The air removal from street canyons ACH_{roof+} estimated by this method was generally consistent with those estimated by the LES models, with differences less than 20% [137].

$$ACH_{roof+} = \frac{1}{\sqrt{6}} \int_A \sqrt{k|_{roof}} \, dA \quad (10)$$

3.2.4. Efficiency of pollutant dispersion

The efficiency of pollutant dispersion can be evaluated by volumetric flow rate (Q), spatially-averaged pollutant concentration (C), purging flow rate (PFR), net escape velocity (NEV), visitation frequency (VF), residence time (TP), age of air (τ_p), and air delay (τ_d). Equations of these indices are listed in Table 4. Except for air delay, the indices were initially proposed for indoor environments. The volumetric flow rate (Q) is the air volume which passes the urban domain per unit time, as defined by Eq. (11) [138]. Although it can largely determine the pollutant dispersion, estimating Q in urban areas is complicated because the spatial wind velocity and cross-sections of the urban domains are highly complex. According to Peng et al., Q is usually limited to investigations of the ventilation efficiency of 2D street canyons and idealized urban geometries [39].

Table 4
Indices of pollutant dispersion efficiency.

Indices	Equation	Variable description
Q [138]	(11) $Q = (\int_A \vec{u} \cdot \vec{n} \, dA)$	\vec{u} : wind velocity vector; \vec{n} : the normal direction of the opening domain surface; A : the area of the opening surface
C [139]	(12) $C = \frac{\int_{Vol} c^* dx dy dz}{Vol}$	c^* : local pollutant concentration; Vol is the volume of the urban domain
PFR [139]	(13) $PFR = \frac{S \times Vol}{C}$	S : uniform pollutant release rate
NEV [140]	(14) $NEV = \frac{PFR}{A_p}$	A_p : whole boundary area of the entire urban volume.
VF [141]	(15) $VF = 1 + \frac{\Delta q}{q} = \frac{\rho \sum_{i=1}^n A_i (uc + u'c')}{Vol \times S}$	Δq : quantity of influx of pollutants into the domain; q : quantity of pollutant emission; A_i : area of face i of inflow boundary; n : total number of faces of the inflow boundary; u : inflow wind speed; u' : velocity fluctuation; c : pollutant concentration; c' : concentration of fluctuation
TP [141]	(16) $TP = \frac{Vol}{PFR \times VF}$	c_p : local pollutant concentration
τ_p [138]	(17) $\tau_p = \frac{c_p}{S}$	τ_p : local mean age of air in the domain with urban geometry; $\tau_{p,empty}$: local mean age of air in the same domain without urban geometry
τ_d [143]	(18) $\tau_d = \tau_p - \tau_{p,empty}$	

Based on the spatial distribution of the pollutant concentration, the spatially-averaged concentration (C) can be calculated by Eq. (12) [139]. However, C alone cannot completely depict the effect of urban fabrics on the pollutant dispersion. PFR, VF, and TP were thus proposed to characterize the dilution, recirculation, and removal of the air pollutant within urban canyons, respectively. PFR estimates the effective airflow rate required to remove the air pollutants from a street, as defined by Eq. (13) [139]. Further, the NEV can be defined by Eq. (14) to estimate the purging flow rate of air pollutants at each unit area [140]. VF represents the number of times a particle enters and passes through an urban domain, as defined by Eq. (15) [141]. TP represents the time needed for a particle to leave the urban domain after its first entry, as defined by Eq. (16) [141].

The local age of air (τ_p) is initially proposed for closed rooms [142]. Applied to urban areas, it represents the time it takes external air in the rural area to reach any location after entering the urban area, as defined by Eq. (17) [138]. In this situation, the external air is assumed to be clean and never return back once departing from a defined domain. By the CFD modelling approach, the value of τ_p is largely dependent on the computational domain and location of the inlet boundary [39]. Therefore, the air delay (τ_d) was proposed to estimate the time delay caused by urban fabrics for the air flow to reach at each location [143]. It is defined as the difference between the τ_p at a certain location in the domain with urban fabrics and that at the same location in an empty domain of the same size, as shown in Eq. (18) [143]. In this way, τ_d is independent of the location of the inlet boundary.

3.3. Methods to assess the temporally-spatially dynamic UTWE

The assessment indices reviewed above can depict the quality of the UTWE at a certain location and moment. However, the UTWE is temporally and spatially dynamic, making it difficult to assess and improve the UTWE in every urban space at all times. Therefore, besides the selection of the assessment indices, the following issues should also be considered when assessing the UTWE:

- 1) Period of interest: the UTWE during which period should be selected for the assessment?
- 2) Which statistical values of the assessment indices are suitable to assess the temporally dynamic UTWE within the period of interest?
- 3) Space of interest: the UTWE from which spaces should be selected for the assessment?
- 4) Which statistical values of the assessment indices are suitable to assess the spatially dynamic UTWE within the space of interest?

These issues can also influence the assessment results of the UTWE. However, systematic suggestions regarding these issues have not been proposed. Therefore, experimental treatments of these issues are summarized from existing studies involving the UTWE assessment on different urban scales.

For the period of interest, the most extreme periods were usually selected to evaluate the thermal environment, and the moments of prevailing wind direction were selected to evaluate the wind environment [87,99,129]. Night-time may be selected for some specific study objectives [144]. To assess the temporally dynamic UTWE, the maximum, minimum, and average of the assessment indices per unit time within a certain period were frequently used in the reviewed studies [12,13,98]. Nazarian et al. proposed three indices to evaluate the percentage of thermal comfort period or average deviation from the thermal comfort condition in the occupied period, including the outdoor thermal comfort autonomy (OTCA), the thermal stress indicator, and the weighted outdoor thermal comfort autonomy [145].

The selection of space of interest usually depends on the urban scale and data source. The general methods to assess the spatially dynamic UTWE on each scale are summarized in Fig. 4. On the micro-scale, the spans of urban spaces are generally less than 500 m, making it

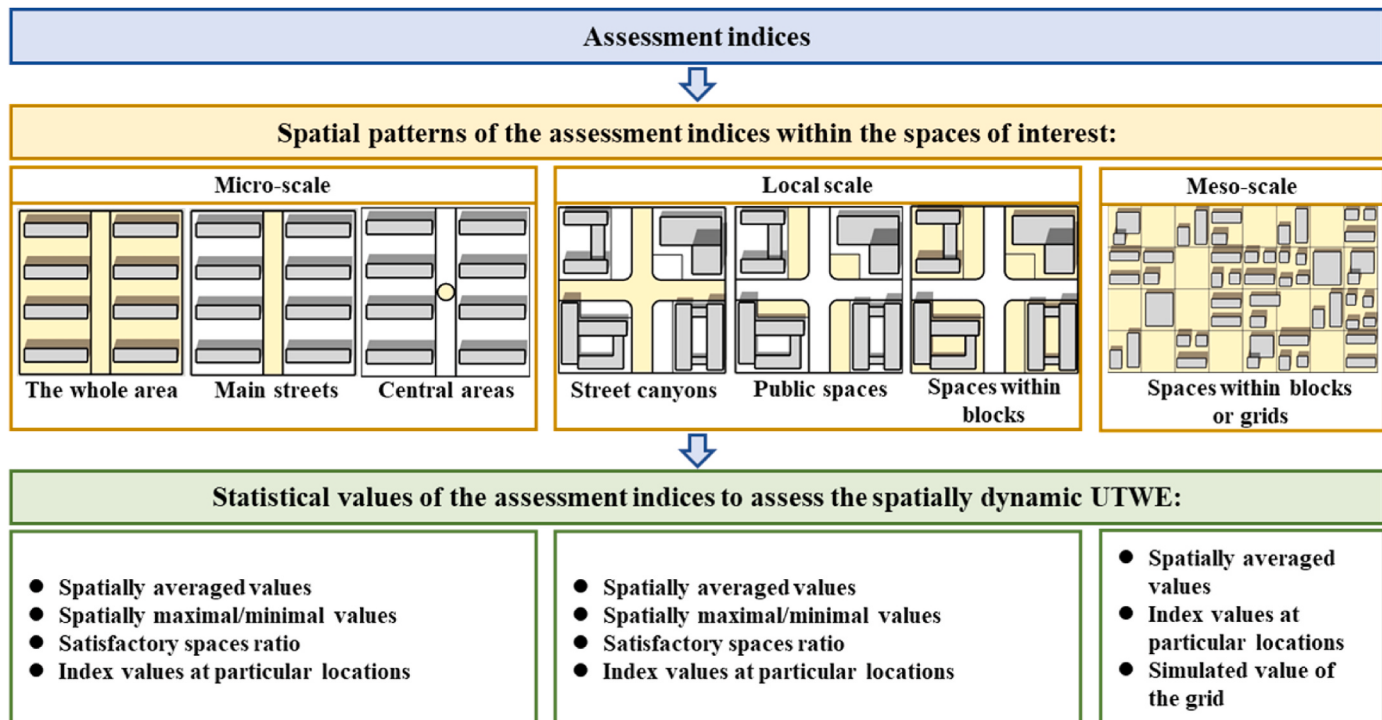


Fig. 4. Procedure to assess the spatially dynamic urban thermal and wind environment (UTWE) on different scales.

convenient to observe the detailed spatial patterns of the assessment indices by means of numerical simulation [20,87]. Through a numerical approach, statistical values such as the average, maximum, and minimum of the assessment indices per unit space were also used to evaluate the overall UTWE of the considered area [87,129,146]. Nazarian et al. proposed spatial and continuous OTCA to evaluate the proportion of thermal comfort areas in the space of interest [145]. The assessment indices at a specific point were also used to represent the UTWE of the surrounding areas [99].

On the local scale, the spaces of interest were certain primary public spaces, such as streets and open squares [12,88,128,129,147–149]. This may be because, with design on this scale, it is difficult to take every detail into account. Through numerical simulation, Shi et al. used the spatial average and the spatial maximum of the wind speed and the AF of several public spaces in a newly designed district to assess their wind environment [129]. Galal et al. used the spatial average PET of different blocks in several urban districts to compare their thermal environment [150]. Wang et al. evaluated the wind environment of a central district by the WVR in the street canyons, and further identified continuous ventilation corridors [61]. Limited by computational capacity, the UTWEs of the public spaces were usually represented by field measurement data when the extent of urban areas exceeded 1 km [12,147].

On the meso-scale, the spaces of interest were usually the blocks and grids of extents from several hundreds of meters to 1 km, which is an efficient way to capture the holistic patterns of the UTWE [17,18,22,97,151–158]. The grid resolution of numerical models on the meso-scale is usually 100 m to 1 km, meaning that the UTWEs are constant within each grid [47,48,94,95]. For data obtained by remote sensing, average land-surface temperatures of the blocks or grids were frequently used to assess their overall thermal environment [152–155]. Through field measurements, the UTWEs of the areas spanning hundreds of meters or several kilometres are represented by the measured data at their centres [11,13,15,33,97,98].

Although there has not been a consensus on how to assess the spatially dynamic UTWE, a reasonable evaluation may be achieved based on the properties of the employed indices and the design and computational cost on different scales. For example, considering the

movement of pedestrians in urban areas, assessing the thermal comfort of the main public activity spaces may be reasonable, but for the assessment of wind security, more urban spaces should be covered to avoid the dangers under gust conditions. In terms of design and computational cost, it is feasible to assess the detailed spatial patterns of the UTWE in the whole designed area on the micro-scale. However, this may be impracticable on the local scale and meso-scale, and focusing on some public spaces, ventilation corridors, and urban cool islands may be more reasonable, considering that the urban planning design on such scales cannot be as elaborate as that on the micro-scale.

3.4. Gaps in the reviewed UTWE-assessment methods on the meso-scale

According to the reviewed literature above, the assessment method of the UTWE on the meso-scale is still needed to be further investigated. The reviewed indices in Section 3.1 and 3.2 only reflect the effect of the UTWE at specific locations or limited domains. Moreover, although some studies assessed the UTWE on the meso-scale by mapping the UTWE of isolated plots or grids as reviewed in Section 3.3, it failed to reflect their interactions which cannot be neglected on such scale. For example, large urban green spaces not only intensify internal cool islands but even extend their cooling effects to the surrounding areas [159–161]. Urban corridors with low roughness can promote the generation of ventilation paths [17,162]. Furthermore, geographical effects also matter on the meso-scale, such as sea breezes in coastal cities and terrains in mountainous cities [17,21,22,158]. Indices such as the UHII, UCII, and WVR can be used to preliminarily identify the spaces of UHIs, UCIs, and ventilation paths, but novel indices or methods should be further proposed to assess the effects of these spaces on the meso-scale.

4. Improvement of the urban thermal and wind environment

One of the primary purposes of modelling and assessing the UTWE is to identify and ameliorate its problems. This section reviews the improvement strategies of the UTWE from three aspects, namely urban morphology, urban green and blue infrastructure, and urban materials. The improvement strategies in each category are analysed in accordance

with the scale on which they are implemented.

4.1. Urban morphology

The UTWE can be significantly influenced by the features of urban morphology. On the micro-scale, the UTWE can be improved by modifying the morphology of street canyons and blocks. On the local scale and meso-scale, controlling the values of morphological parameters of each block is also considered to avoid unsatisfactory UTWE. Further, reserving ventilation corridors can be used as an efficient way to improve the ventilation on the local scale and meso-scale. Studies about these strategies are reviewed in this section.

4.1.1. Strategies on the micro-scale

On the micro-scale the strategies for urban morphology focus on the geometry of street canyons and blocks. Understanding their effects on the UTWE is the foundation for implementing efficient design strategies. In street canyons, the aspect ratio and street orientation both influence the UTWE. Although narrow streets obstruct heat dissipation during night-time, its cooling effect during daytime was found to be more significant [163,164]. The shading effects of deep streets provide lower temperatures and improve thermal comfort during daytime [163,165, 166].

The thermal effect of the aspect ratio also depends on the street orientation. East-West (E-W)-oriented streets experience more prolonged exposure to direct solar radiation than streets in other orientations [167]. Increasing the aspect ratio of E-W-oriented streets is less efficient than increasing that of North-South (N-S)-orientated streets to improve thermal comfort [166]. However, at noon time, the PET in N-S-oriented streets can be only slightly lower than that in E-S-oriented streets because of the high solar altitude [168]. The south side of E-W-oriented deep streets may be even more comfortable due to shadows at noon [147]. In comparison, streets in intermediate orientations are always partially shaded and offer an alternative for pedestrians [167]. When the wind direction is parallel to the street axis, an obstacle-free air path can be developed [30]. However, when it is perpendicular to the street axis, a stable canyon vortex is developed after the aspect ratio exceeds 0.7 [169].

We note that most of the case studies above were carried out for relatively continuous street canyons. The aspect ratio of the street with detached buildings was found to have little influence on outdoor thermal comfort [170]. The UTWEs were significantly correlated with spatial morphology features within a range of several hundred meters in radius [11–13]. Some morphological parameters at the block level were found to be more decisive for the pedestrian UTWE, mainly including building coverage ratio (BCR), building height (BH), sky view factor (SVF), roughness length (RL), frontal area index (FAI), and frontal area density (FAD) [11–17].

The BCR, BH, and SVF can influence the urban thermal environment. Several studies have confirmed that the BCR and BH have positive effects on the nocturnal air temperature or UHII [11,15]. However, during daytime, increasing the BCR and BH not only reduces cooling efficiency and causes multiple reflection, but also provides shadows to reduce heat absorption [171]. Therefore, the effects of BCR and BH on the daytime air temperature can be more complex and were reported as positive, negative, or insignificant by different studies [12–15]. The SVF represents the proportion of visible sky at a specific location, which controls the amount of global radiation in daytime and the radiative cooling during night-time [11,171]. Positive effects of SVF on daytime temperature and negative effects of SVF on nocturnal temperature were found in Hong Kong [9]. However, the correlations between SVF and air temperature tend to be insignificant within entire urban areas containing various land-uses [172], and weakened by the advective effects from the wider environment [173].

Compared with the three parameters above, the RL, FAI, and FAD are more influential for the urban wind environment because they reflect

the wind resistance of a building cluster in different wind directions. The RL is tightly connected to the turbulence in the roughness sublayer and affects wind velocity over surfaces [174,175]. A negative correlation between RL and wind speed was also reported [33]. Compared with the RL, the FAI and FAD can be more controllable in the design stage. The FAI is defined as the windward building area per unit site's area (Fig. 5a), and FAD can be deemed the FAI value for a specified height increment (Fig. 5b) [16]. They are both negatively correlated to wind speed [16,33]. Compared with the FAI, which describes the wind resistance of the entire urban canopy, FAD represents the aerodynamic effect of the respective height level [16]. The FAD within a height increment of 0–15 m was found to have a stronger effect on wind speed at the pedestrian level than for other height increments in Hong Kong [16].

Several design strategies for the urban morphology on the micro-scale are listed in Table 5 to provide references for the urban planning design. However, it should be noted that the applicability of each suggestion is influenced by regional factors, such as the latitude, solar altitude, climate characteristic, terrain, and elevation. Further, limited by the research methods employed and cases studied, the results may be one-sided considering the complex correlation between urban morphology and the UTWE as mentioned above. Achieving optimal improvement strategies also calls for the iterative modification and assessment of different design scenarios [20].

4.1.2. Strategies on the local scale and meso-scale

On the local scale and meso-scale, modifying the aforementioned morphological parameters for each block is also suitable. Furthermore, arrays of blocks with low wind resistance were found to generate ventilation corridors, which improve ventilation and induce cooler and cleaner air flow from the suburbs on the urban scale (Fig. 6) [17,178]. Guo et al. found that within the ventilation corridors, the average FAIs ranged from 0.18 to 0.62 and the average wind velocities were improved by 12%–52% compared with the surroundings [21]. Grunwald et al. further employed numerical simulations and particle track analyses to map cold-air paths, which were of low-roughness, and linked cold-air sources and warmer areas [179]. Low terrain elevations and low-rise buildings were found to increase the occurrences of cold-air paths [180].

Several criteria for ventilation corridor design have been proposed in terms of urban morphology and air sources. The essential principle is to ensure nearly straight free paths to the urban centre, whose surfaces should be low in roughness, cool the passing air, and avoid pollution [181]. Mayer et al. proposed elaborate design criteria for the ventilation corridors and limited the surface roughness length to 0.5 m [178,182]. However, Grunwald et al. suggested that these criteria may be too strict, because regions with higher roughness were also found to generate air paths [179]. Ren et al. further distinguished major ventilation corridors and secondary corridors, and proposed different levels of roughness lengths and air sources for each kind of corridor [17].

On the local scale, it is better to focus especially on the pedestrian ventilation path (Fig. 6). Wang et al. identified pedestrian-level ventilation paths based on the spatial patterns of the WVR, and the identified ventilation paths were open spaces or street canyons along the prevailing wind direction [61]. The air flow within street canyons can be channelled along the axis when the angle is less than 30° [29,61]. He et al. stated that the street structure also influences the ventilation potential on the local scale, and the gridiron pattern was deemed the most efficient pattern [29]. Galal et al. suggested modifying the patterns of street networks to reduce adverse street orientations [150].

4.2. Urban green and blue infrastructure

The urban green and blue infrastructure consists of vegetation and water bodies, including natural and designed landscape components [183]. Vegetation includes street trees and green spaces such as parks, grass lands and urban forests, while the water bodies include fountains

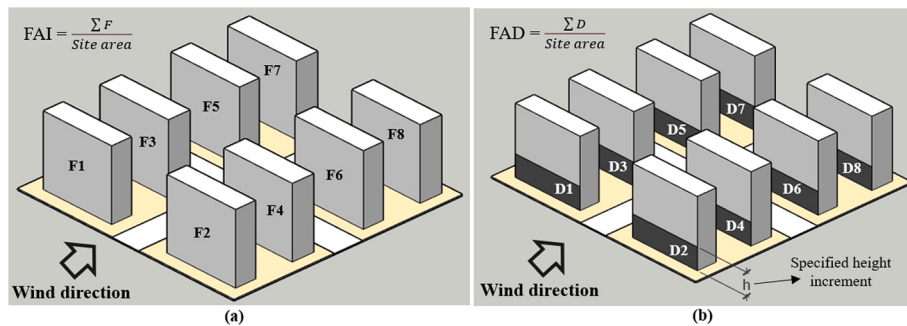


Fig. 5. Illustration of the calculation methods: (a) frontal area index (FAI), and (b) frontal area density (FAD).

Table 5
Design strategies about the urban morphology on micro-scale.

Morphological parameters	Design strategy	Region of the study case
Aspect ratio	1. Increasing the aspect ratio to decrease the maximum temperature [163]. 2. Reducing the aspect ratio to improve the nocturnal cooling rate [176].	1. Fez, Morocco 2. Athens, Greece.
Street orientation	1. The aspect ratio of E-W-oriented streets needs to reach 3.0 to achieve satisfactory thermal comfort. For N-S-oriented streets, aspects exceeding 0.6 can supply satisfactory thermal comfort for most of the day. For aspect ratios exceeding 2.0, the thermal comfort in N-S-oriented streets is similar to that in diagonal streets [166]. 2. When the street is perpendicular to the wind direction, the aspect ratio should be less than 0.7 to avoid stable canyon vortex [169].	1. Tinos, Greece
Building coverage ratio	1. Increasing BCR by 10% leads to a 0.91 °C increase in the daytime maximal temperature, and 0.77 °C increase in the nocturnal maximal UHII [98].	1. Foshan, China
Building height	1. Increasing BH by 10 m leads to about a 1.9 °C increase in the nocturnal maximal UHII in summer [11]. 2. With the BCR of 50%, increasing the BH from 14 m to 24 m decreases air temperature by 3.68 °C at 1:00 p.m. [14].	1. Rotterdam, Netherlands 2. Milan, Genoa, and Rome.
Sky view factor	1. Increasing SVF by 0.1 decreases the mean nocturnal temperature by about 0.38 °C [177]. 2. Decreasing SVF by 0.2 reduces daytime UHII by 0.3 °C, and increases nocturnal UHII by 0.1 °C [10].	1. Hong Kong 2. Shanghai, China
Roughness length	1. The RL should be lower than 0.5 to maintain relatively high potential wind dynamics [17].	
Frontal area index	1. A 10% increase in FAI reduces about 0.22 m/s of the annual average wind speed [33].	1. Beijing, China
Frontal area density	1. The FAD within the height increment of 0–15 m has the strongest effect on wind speed at the pedestrian level. Decreasing the FAD from 0.47 to 0.35 significantly improved the wind environment at the pedestrian level [16].	1. Hong Kong

and blue spaces such as lakes, rivers, and wetlands. On the micro-scale, the street trees can improve the surrounding thermal comfort by the shading effect. On the local scale and meso-scale, the green and blue spaces can generate urban cool islands and further extend the cooling effects to the surrounding urban areas. Studies about these strategies are reviewed in this section.

4.2.1. Strategies on the micro-scale

On the micro-scale, the cooling effect of street trees is more efficient than that of grassland and water bodies due to their shading effect. Grasslands alone reduce the diurnal average PET by only 1 °C in summer [184]. Water fountains in Southwest Germany can reduce the surrounding PET by 1.4 °C in the summer afternoon [185]. In comparison, street trees can reduce the diurnal average PET by as much as 3 °C in summer [184]. Adding dense tree covers on grass lawns was found to reduce the daytime PET by 15 °C in Shanghai, China [186].

The number of trees needed to provide an effective cooling effect on the micro-scale is a key question. Ng et al. suggested that 33% of green covers are needed to reduce the air temperature by 1 °C in Hong Kong [187]. However, the cooling effect of street trees also depends on the form of the street canyon they are in. The shading effect of buildings may complement and even exceed that of trees, especially in deep canyons [188]. The cooling potential of trees in low-rise urban areas tends to be greater than that in high-rise areas [187]. The cooling effect of trees along E-W-oriented streets was found to be more evident than that along N-S-oriented streets [166]. Therefore, Norton et al. proposed four priority levels for street greening based on the width, height, and orientation of the streets [189]. The E-W-oriented streets with the highest greening priorities are those whose aspect ratios are less than 1.0, while for the N-S-oriented streets, increasing their aspect ratios to 0.3 can change their greening priorities from the highest to moderate [189].

The shape of trees also has an impact on their cooling effect. Milošević et al. suggested that cylinder-shaped tree crowns can mitigate heat stress more effectively than sphere-shaped and cone-shaped crowns of the same height and diameter [190]. Leaf area index (LAI) is an important parameter related to the shelter effect of trees. A higher LAI means a larger ratio of leaf area to ground cover, and thus a larger radiation reduction [191,192]. The cooling potential of trees with dense foliage is limited in deep canyons, but can trap long-wave radiation and block ventilation [193]. Morakinyo et al. proposed a scheme for selecting proper tree species for urban canyons with different SVFs [188]. When SVFs are less than 0.2, tall trees with sparse to moderate foliage density and high trunk were recommended; short trees with moderate foliage density and high trunk were recommended when SVFs range between 0.2 and 0.45; and for urban canyons with the SVFs greater than 0.45, short trees with dense foliage and high trunk were recommended [188].

4.2.2. Strategies on the local scale and meso-scale

On the local scale and meso-scale, urban green and blue spaces can generate urban cool islands and extend their cooling effects to the



Fig. 6. Major ventilation corridors over urban blocks and air path within street canyons.

surrounding areas. The maximal temperature difference between a garden and its sounding streets reached 6.9 °C in Lisbon [194]. The air temperature and surface temperature near water bodies were reported to be 2.2 °C and 3.32 °C lower respectively than their surroundings [195, 196]. The cooling effects of green and blue spaces can extend tens of meters to exceeding 1 km to the surrounding areas [159–161, 196–198], depending on their size, composition, and configuration.

Generally, increasing the sizes of green and blue spaces can improve their cooling effects [159, 199–203]. However, once the size of the green and blue spaces exceeds a certain threshold value, defined as the threshold value of efficiency (TVoE), the improvement of their cooling effects can become negligible and their cooling efficiency of per unit area thus decreases [161]. Identifying the TVoE can allow a trade-off between ecological effects and land economy. According to a review of Yu et al. [43], the proposed TVoE values of green and blue spaces are inconsistent across cities. For green spaces, the TVoE was reported to be 3 ha in Taipei [204], 0.69 ha in Copenhagen [205], and 0.6–0.95 ha in low-latitude-Asian cities [206]. For blue spaces, the TVoE was reported to be 1.12 ha in Copenhagen [205]. In the same city, increase in the background temperature can decrease the cooling efficiency of the green spaces and increase their TVoE [206].

The composition of green spaces, described by the contained landscape types and their proportions [207], can also influence the TVoE by determining the cooling efficiency per unit area of green spaces. The cooling efficiency of green spaces due to trees and shrubs can be higher than those made up of grass [208]. Increasing the forest vegetation in green spaces can intensify the UCII [199] and extend the cooling distance [209]. Quantitative indices such as the normalized difference vegetation index, leaf area index, and woody vegetation ratio were found to be negatively related to the UCII [210–212].

Besides the size and composition, the configuration also influences the cooling effect of green and blue spaces. Configuration describes the spatial characteristics and spatial relationships among landscapes [207]. For green spaces, the configuration was found to explain 6–12% of the land surface temperature [213]. Complex configurations, featured by

aggregated patch shapes and irregular patch edges, were recommended to intensify the cooling effects of green spaces [159, 199–201, 212, 214]. Fragmented green spaces with irregular shapes provide more shadows and interfaces with their surroundings for heat exchange [43, 212, 214]. However, increasing the complexity of green spaces does not always improve their cooling effects. Jaganmohan et al. found that the complexity was negatively correlated with the cooling effects of the green spaces when the sizes were less than 5.6 ha [215]. This may be explained by the fact that larger green spaces tend to generate a more stable microclimate [43]. In terms of blue spaces, their cooling intensities were reported to be negatively related to the landscape shape index [203] and decreased by fragmented shapes [202].

4.3. Strategies on materials

To reduce the solar radiation absorbed by urban surfaces, reflective materials are considered a strategy to mitigate the UHI. The maximal difference in the surface temperature reached around 9 °C among three pavements with albedo ranging from 0.21 to 0.38 on a summer day [185]. The ambient temperature can be reduced by 1.5 °C when reflective pavement is used on a major traffic axis on a large scale [216]. When the reflective materials are used on roofs, the cooling effect at the pedestrian level may be diminished with the increase in building height [42]. Although the reflective materials can reduce the air temperature, their effect on increasing the mean radiation temperature may be more evident, which exacerbates thermal comfort [42]. Increasing the pavement albedo by 0.4 can increase the mean radiation temperature by 10.53 °C and the PET by 4.7 °C [217]. Furthermore, the cooling effect of reflective pavement was found to be larger around medium-rise buildings than around high-rise buildings [218]. Qin et al. suggested using reflective pavements when the aspect ratio of streets is not greater than 1.0 [219].

Besides reflective materials, evaporative pavements are also used to mitigate the UHI, which include porous pavement, permeable pavement, pervious pavement, and water-retaining pavements [220]. Porous

pavement consists of cellular grids with internal holes for permeating water [220]. A study in Japan indicated that porous pavements filled with grass reduced daytime sensitive heat flux by approximately 100–150 W m⁻² and nocturnal sensitive heat flux by approximately 50 W m⁻² compared with asphalt surface [221]. Permeable pavement is composed of a layer of bricks that are separated by small openings or spacing lugs allowing water to pass around and evaporate; while the pervious pavement is a special kind of concrete with a high porosity allowing water to pass directly through it [220]. The permeable pavement and pervious pavement both require wet conditions for evaporative cooling effect. Ferrari et al. recommended a double-layer pervious pavement of which the top layer consists of finer material and the bottom layer consists of coarser material to achieve optimal evaporative cooling [222]. Kubilay et al. further proposed an artificially watering schedule to maximize the evaporative cooling effect of the double-layer pervious pavement [223]. To retain the water for evaporative cooling, water-retaining pavement is developed by embedding water-retentive fillers in the concrete [220]. Nakayama and Fujita reported that the air temperature above the water-retaining pavement was 3–5 °C lower than that above the building rooftop [224].

4.4. Interdependences among influential factors of the UTWE

According to the reviewed literature above, it is noted that the effects of many urban design factors on the UTWE are not consistent but interdependent. Such interdependent thermal effects have been found among the orientation, aspect ratio and greening of the streets, and the scale, composition and configuration of the green spaces in this review. Similarly, the cooling effect of street trees and reflective materials were also reported to be dependent on the street morphologies [42]. The interdependences among the influential factors indicate that the UTWE is not simply influenced by a linear cumulative effect of these factors, but by a complex coupling effect of them. However, such a complex coupling effect may be simplified by some studies due to the use of bivariate linear regression analysis or neglecting to control variations of the design factors. As a result, some of the conclusions about urban design strategies to improve the UTWE from different studies are still contradictory, which should be highly noticed.

5. Discussion

5.1. Effect of urban scale on UTWE studies

It is clear that the scale plays an important role in modelling, assessing, and improving the UTWE. With regard to modelling, the simplification of the Navier-Stokes equation and treatment of urban geometry for CFD models and meso-scale models are different [34]. The CFD models for micro-scale and local scale mostly do not consider the atmospheric interactions such as atmospheric vertical mixing or Coriolis effect as meso-scale models [34]. However, the CFD models simulate the UTWE on the micro-scale and local scale with actual urban geometrical models by fine resolution. The meso-scale models and UCMs simulate the UTWE using descriptive parameters of urban geometries and ground surfaces by coarse resolution. This approach is partly driven by considerations of computational cost and the required accuracy on the meso-scale. Simulating the UTWE on the meso-scale using actual urban geometrical models may be too computationally intensive and time-consuming. In addition, detailed information on the UTWE that can only be acquired at a fine resolution is less of a concern on the meso-scale.

With regard to assessing the spatially dynamic UTWE, no clear consensus emerged from the literature review. However, some similar methods can be summarized by this review. On the micro-scale, the entire space in the considered area can be a space of interest, and the CFD simulation with fine resolution makes it possible to assess the detailed spatial patterns of the UTWE. On the local scale, the spaces of

interest are usually the streets and public activity spaces in the considered area rather than the entire area, considering that improving every undesirable area can be hard for design practice. Statistical values of the assessment indices within the spaces of interest are usually used to evaluate the UTWE, which is more efficient than observing the spatial patterns of these indices when large spaces are considered. On the meso-scale, the UTWEs are usually assessed with coarse resolution covering hundreds of meters, which is an efficient way to capture the overall UTWE features of a city.

With regard to improving the UTWE, the strategies applied on each scale can be differentiated by theoretical and practical factors. On the micro-scale, the spatial morphology and vegetation arrangement can be exquisitely modified to adjust the solar radiation and advection at specific locations. On the local scale and the meso-scale, the configuration of urban blocks and green-blue spaces are considered because they can impact the UTWE over wider areas by generating ventilation corridors or urban cool islands. The morphology of blocks within a district or city can be modified by morphological parameters instead of actual geometries to improve design efficiency. In comparison with the meso-scale, the structure of street networks can receive closer attention on the local scale to improve the ventilation on the pedestrian level.

5.2. Challenges and opportunities

As illustrated in Fig. 1, consideration of the UTWE in urban planning design is systematically composed of its modelling, assessment, and improvement. Current studies can generally support the three steps, in terms of modelling tools and corresponding guidelines, basic assessment indices, and principles of improvement strategies of the UTWE, although some of them are still needed to be improved to adapt to different scales and conditions as discussed in Section 2.2.1, 3.4, and 4.4.

However, when systematically considering the progress of the modelling, assessment, and improvement of the UTWE, more challenges should be highlighted. Firstly, in terms of the UTWE modelling technologies, their efficiencies play an important role in urban planning design. Although the CFD models are relatively reliable methods, they require high computational costs. Secondly, although the current studies provide basic principles of urban and landscape design to improve the UTWE, some specific conclusions are still limited by the research methods, selected urban sites, and geographical locations. Currently, achieving optimal urban design scenarios still require iterative modifications and simulations, which also stresses the importance of modelling efficiency. Last but not least, the UTWE assessment is supposed to provide sufficient information for the improvement steps. However, based on the current assessment indices and methods, proposing suitable design schemes to improve the UTWE still depends on individual experiences, and novel methods are needed as a link between the two steps. The following sections further provide insights for future studies about these issues.

5.2.1. Efficiency of the UTWE models for urban planning design

Improvements in the UTWE usually involve repetitive modification and simulation to achieve relatively optimal design scenarios. In recent years, the simulation tools have been further integrated with intelligent algorithms for optimizing architecture and urban design [225–228]. These methods may not be feasible if the application of inefficient models leads to extensive computational loads. Therefore, developing efficient models should also be concerned. To improve the UTWE, simulation models are used to compare the UTWE for different design scenarios. Therefore, the models need to reflect the relative differences among the UTWEs of different scenarios, but not necessarily reflect absolutely accurate results. From this point of view, empirical models may be suitable alternatives to the CFD models for optimization design. Empirical models considering comprehensive effects of urban form on the UTWE can be much more efficient than CFD models. Several studies have attempted to employ machine learning approaches to develop

empirical models to predict the UTWE [229,230]. More factors may be involved to develop more accurate but efficient empirical models in the future.

5.2.2. Resolving coupling effects of the influential factors on the UTWE

Understanding the correlation between urban design factors and the UTWE is the foundation to achieving efficient design strategies. However, as discussed in Section 4.4, influential factors of the UTWE are interdependent. Some commonly used methods such as regression analysis cannot further resolve the coupling effects of multiple factors on the UTWE. Some advanced models are needed to be involved in this research field. For example, a rule-based effect of building density and building height on the land surface temperature was constructed by Guo et al. using rule-based regression [154]. Meanwhile, the methodology of urban typology is also helpful to resolve the coupling effects of multiple urban design factors. The Local Climate Zone scheme of Stewart and Oke can be a classic typology to study urban climate. This scheme classified urban constructions and landscapes into 17 types according to their morphological features and thermal performances [100]. On this basis, variational correlations between land surface temperature and building height among different LCZs were recently reported by Yang et al. [231].

5.2.3. Linking the assessment and improvement of the UTWE

Currently, assessment methods of the UTWE cannot directly guide the improvement design. Firstly, the standards of many assessment indices of the UTWE are unclear, which makes it ambiguous to decide whether a design scenario should be modified. Meanwhile, due to the limitations to understanding the coupling effects of the design factors on the UTWE, choosing the most influential design factors for a specific design scenario also calls for professional knowledge.

To solve these problems, urban typology such as the Local Climate Zone may also provide a suitable scheme. Although the UTWEs of some LCZs are intrinsic worse than the others, they are inevitable in realistic cities to provide specific functions. Meanwhile, adjusting the urban configurations of the same LCZs can also lead to differences in their UTWE [232]. Therefore, understanding the ranges of the UTWE-indices of each LCZ type can be firstly helpful to determine their standards. In this way, the worse UTWE of an urban scenario compared with those of its same LCZs indicates that there is potential for it to be improved. On this basis, investigating the effects of design factors on the UTWE of different LCZs can help to determine the most influential factors for an urban scenario.

The development of data-driven approaches also provides the opportunity to link the assessment and improvement of the UTWE. These approaches have been applied to optimizing building energy efficiency, which detects problematic design parameters based on a database of architectural parameters and energy consumption, and statistical and machine learning models [233]. However, this approach has been less used for the optimization of urban design. This may be explained by the fact that urban forms are usually too complex to be comprehensively described by quantitative parameters, and the on-site climate data are still not sufficient to employ data-driven optimization.

6. Conclusion

Consideration of the UTWE involves multiple scales. A review was conducted of the modelling, assessment, and improvement methods of the UTWE on different scales. The purpose was to investigate the effect of urban scale on the application of these methods and clarify the limitations of current methods based on the requirement of each step and the phenomenon of the UTWE on each scale. A comprehensive insight into the methods to simulate, assess, and improve the UTWE in urban planning design can also result from this review. The principal findings are as follows.

- 1) Progress of the reviewed studies can generally support the modelling, assessment, and improvement of the UTWE in urban planning design. The UTWE modelling methods include CFD models and meso-scale models which can be integrated with the UCMs. The reviewed assessment indices cover aspects of the UHI, natural ventilation, and thermal and wind comfort. The UTWE can be improved by modifying the street/block morphology and street trees on the micro-scale, reserving the ventilation corridors and the green and blue spaces on the local scale and meso-scale, and using reflective and evaporative pavement.
- 2) The research scale was generally considered by studies of the modelling and improvement of the UTWE because it is closely related to the dominant influential factors of the UTWE. However, studies of UTWE assessment have not considered the research scale theoretically. On the meso-scale, the UTWE of plot units are usually evaluated in isolation and the interactions among them are neglected.
- 3) Some conclusions about the UTWE improvement strategies still contradict each other. The effects of many influential factors of the UTWE are interdependent, which was found among the orientation, aspect ratio and greening of the streets, and the scale, composition and configuration of the green spaces. Urban typology such as the Local Climate Zone provides an efficient scheme to further investigate the coupling effects of multiple factors on the UTWE.
- 4) Current assessment methods of the UTWE cannot directly guide the improvement design because of the ambiguous assessment standard and limitation in identifying the most influential factors for a specific design scenario. The data-driven approaches provide an opportunity to link the assessment results and corresponding improvement strategies.

CRediT authorship contribution statement

Sihong Du: Writing – review & editing, Writing – original draft, Visualization, Validation, Methodology, Investigation, Formal analysis, Data curation, Conceptualization. **Xinkai Zhang:** Writing – review & editing, Data curation. **Xing Jin:** Supervision, Writing – review & editing. **Xin Zhou:** Writing – review & editing, Supervision. **Xing Shi:** Supervision, Writing – review & editing.

Declaration of competing interest

The authors declare that they have no known competing financial interests or personal relationships that could have appeared to influence the work reported in this paper.

References

- [1] U. Nations, *World Urbanization Prospects: the 2018 Revision*, UN DESA, New York, USA, 2018.
- [2] T.R. Oke, *Boundary Layer Climate*, Methuen, London, UK, 1987.
- [3] Y. Liu, Q. Li, L. Yang, K. Mu, M. Zhang, J. Liu, Urban heat island effects of various urban morphologies under regional climate conditions, *Sci. Total Environ.* 743 (2020) 140589, <https://doi.org/10.1016/j.scitotenv.2020.140589>.
- [4] Y. Wang, Z. Guo, J. Han, The relationship between urban heat island and air pollutants and them with influencing factors in the Yangtze River Delta, China, *Ecol. Indicat.* 129 (2021), <https://doi.org/10.1016/j.ecolind.2021.107976>.
- [5] M. Santamouris, On the energy impact of urban heat island and global warming on buildings, *Energy Build.* 82 (2014) 100–113, <https://doi.org/10.1016/j.enbuild.2014.07.022>.
- [6] L.P. Wong, H. Alias, N. Aghamohammadi, S. Aghazadeh, N.M. Nik Sulaiman, Urban heat island experience, control measures and health impact: a survey among working community in the city of Kuala Lumpur, *Sustain. Cities Soc.* 35 (2017) 660–668, <https://doi.org/10.1016/j.scs.2017.09.026>.
- [7] J. Taylor, P. Wilkinson, M. Davies, B. Armstrong, Z. Chalabi, A. Mavrogiani, P. Symonds, E. Oikonomou, S.I. Bohnenstengel, Mapping the effects of urban heat island, housing, and age on excess heat-related mortality in London, *Urban Clim.* 14 (2015) 517–528, <https://doi.org/10.1016/j.uclim.2015.08.001>.
- [8] G.S. Golany, Urban design morphology and thermal performance, *Atmos. Environ.* 30 (1996) 455–465.

- [9] R. Giridharan, S.S.Y. Lau, S. Ganesan, B. Givoni, Urban design factors influencing heat island intensity in high-rise high-density environments of Hong Kong, *Build. Environ.* 42 (10) (2007) 3669–3684, <https://doi.org/10.1016/j.buildenv.2006.09.011>.
- [10] F. Yang, S.S.Y. Lau, F. Qian, Urban design to lower summertime outdoor temperatures: an empirical study on high-rise housing in Shanghai, *Build. Environ.* 46 (3) (2011) 769–785, <https://doi.org/10.1016/j.buildenv.2010.10.010>.
- [11] L.W.A. van Hove, C.M.J. Jacobs, B.G. Heusinkveld, J.A. Elbers, B.L. van Driel, A. A.M. Holtslag, Temporal and spatial variability of urban heat island and thermal comfort within the Rotterdam agglomeration, *Build. Environ.* 83 (2015) 91–103, <https://doi.org/10.1016/j.buildenv.2014.08.029>.
- [12] S. Tong, N.H. Wong, S.K. Jusuf, C.L. Tan, H.F. Wong, M. Ignatius, E. Tan, Study on correlation between air temperature and urban morphology parameters in built environment in northern China, *Build. Environ.* 127 (2018) 239–249, <https://doi.org/10.1016/j.buildenv.2017.11.013>.
- [13] D. Xu, D. Zhou, Y. Wang, W. Xu, Y. Yang, Field measurement study on the impacts of urban spatial indicators on urban climate in a Chinese basin and static-wind city, *Build. Environ.* 147 (2019) 482–494, <https://doi.org/10.1016/j.buildenv.2018.10.042>.
- [14] K. Perini, A. Magliocco, Effects of vegetation, urban density, building height, and atmospheric conditions on local temperatures and thermal comfort, *Urban For. Urban Green.* 13 (3) (2014) 495–506, <https://doi.org/10.1016/j.ufug.2014.03.003>.
- [15] Y. Lan, Q. Zhan, How do urban buildings impact summer air temperature? The effects of building configurations in space and time, *Build. Environ.* 125 (2017) 88–98, <https://doi.org/10.1016/j.buildenv.2017.08.046>.
- [16] E. Ng, C. Yuan, L. Chen, C. Ren, J.C.H. Fung, Improving the wind environment in high-density cities by understanding urban morphology and surface roughness: a study in Hong Kong, *Lands. Urban Plann.* 101 (1) (2011) 59–74, <https://doi.org/10.1016/j.landurbplan.2011.01.004>.
- [17] C. Ren, R. Yang, C. Cheng, P. Xing, X. Fang, S. Zhang, H. Wang, Y. Shi, X. Zhang, Y.T. Kwok, E. Ng, Creating breathing cities by adopting urban ventilation assessment and wind corridor plan – the implementation in Chinese cities, *J. Wind Eng. Ind. Aerod.* 182 (2018) 170–188, <https://doi.org/10.1016/j.jweia.2018.09.023>.
- [18] C. Ren, K.L. Lau, K.P. Yiu, E. Ng, The application of urban climatic mapping to the urban planning of high-density cities: the case of Kaohsiung, Taiwan, *Cities* 31 (2013) 1–16, <https://doi.org/10.1016/j.cities.2012.12.005>.
- [19] B. Blocken, W.D. Janssen, T. van Hooff, CFD simulation for pedestrian wind comfort and wind safety in urban areas: general decision framework and case study for the Eindhoven University campus, *Environ. Model. Software* 30 (2012) 15–34, <https://doi.org/10.1016/j.envsoft.2011.11.009>.
- [20] M.P. Heris, A. Middel, B. Muller, Impacts of form and design policies on urban microclimate: assessment of zoning and design guideline choices in urban redevelopment projects, *Lands. Urban Plann.* 202 (2020), <https://doi.org/10.1016/j.landurbplan.2020.103870>.
- [21] F. Guo, H. Zhang, Y. Fan, P. Zhu, S. Wang, X. Lu, Y. Jin, Detection and evaluation of a ventilation path in a mountainous city for a sea breeze: the case of Dalian, *Build. Environ.* 145 (2018) 177–195, <https://doi.org/10.1016/j.buildenv.2018.09.010>.
- [22] X. Zhou, T. Okaze, C. Ren, M. Cai, Y. Ishida, H. Watanabe, A. Mochida, Evaluation of urban heat islands using local climate zones and the influence of sea-land breeze, *Sustain. Cities Soc.* 55 (2020), <https://doi.org/10.1016/j.scs.2020.102060>.
- [23] M. Pacifici, F. Rama, K.R. de Castro Marins, Analysis of temperature variability within outdoor urban spaces at multiple scales, *Urban Clim.* 27 (2019) 90–104, <https://doi.org/10.1016/j.uclim.2018.11.003>.
- [24] P.M. Schirmer, K.W. Axhausen, A multiscale classification of urban morphology, *J. Transport Land Use* (2015), <https://doi.org/10.5198/jtlu.2015.667>.
- [25] T. Yamada, K. Koike, Downscaling mesoscale meteorological models for computational wind engineering applications, *J. Wind Eng. Ind. Aerod.* 99 (4) (2011) 199–216, <https://doi.org/10.1016/j.jweia.2011.01.024>.
- [26] A. Mochida, S. Iizuka, Y. Tominaga, I.Y.-F. Lun, Up-scaling CWE models to include mesoscale meteorological influences, *J. Wind Eng. Ind. Aerod.* 99 (4) (2011) 187–198, <https://doi.org/10.1016/j.jweia.2011.01.012>.
- [27] N.H. Wong, Y. He, N.S. Nguyen, S.V. Raghavan, M. Martin, D.J.C. Hii, Z. Yu, J. Deng, An integrated multiscale urban microclimate model for the urban thermal environment, *Urban Clim.* 35 (2021), <https://doi.org/10.1016/j.uclim.2020.100730>.
- [28] N. Lauzet, A. Rodler, M. Musy, M.-H. Azam, S. Guernouti, D. Mauree, T. Colinart, How building energy models take the local climate into account in an urban context – a review, *Renew. Sustain. Energy Rev.* 116 (2019), <https://doi.org/10.1016/j.rser.2019.109390>.
- [29] B.-J. He, L. Ding, D. Prasad, Enhancing urban ventilation performance through the development of precinct ventilation zones: a case study based on the Greater Sydney, Australia, *Sustain. Cities Soc.* 47 (2019), <https://doi.org/10.1016/j.scs.2019.101472>.
- [30] E. Jamei, P. Rajagopalan, M. Seyedmahmoudian, Y. Jamei, Review on the impact of urban geometry and pedestrian level greening on outdoor thermal comfort, *Renew. Sustain. Energy Rev.* 54 (2016) 1002–1017, <https://doi.org/10.1016/j.rser.2015.10.104>.
- [31] X. Luan, Z. Yu, Y. Zhang, S. Wei, X. Miao, Z.Y.X. Huang, S.N. Teng, C. Xu, Remote sensing and social sensing data reveal scale-dependent and system-specific strengths of urban heat island determinants, *Rem. Sens.* 12 (3) (2020), <https://doi.org/10.3390/rs12030391>.
- [32] S. Du, Y. Li, C. Wang, Z. Tian, Y. Lu, S. Zhu, X. Shi, A cross-scale Analysis of the correlation between daytime air temperature and heterogeneous urban spaces, *Sustainability* 12 (18) (2020), <https://doi.org/10.3390/su12187663>.
- [33] Y. Liu, Y. Xu, F. Weng, F. Zhang, W. Shu, Impacts of urban spatial layout and scale on local climate: a case study in Beijing, *Sustain. Cities Soc.* 68 (2021), <https://doi.org/10.1016/j.scs.2021.102767>.
- [34] P.A. Mirzaei, F. Haghhighat, Approaches to study urban heat island – abilities and limitations, *Build. Environ.* 45 (10) (2010) 2192–2201, <https://doi.org/10.1016/j.buildenv.2010.04.001>.
- [35] Y. Toparlar, B. Blocken, B. Maiheu, G.J.F. van Heijst, A review on the CFD analysis of urban microclimate, *Renew. Sustain. Energy Rev.* 80 (2017) 1613–1640, <https://doi.org/10.1016/j.rser.2017.05.248>.
- [36] S. Tsoka, A. Tsikaloudaki, T. Theodosiou, Analyzing the ENVI-met microclimate model's performance and assessing cool materials and urban vegetation applications—A review, *Sustain. Cities Soc.* 43 (2018) 55–76, <https://doi.org/10.1016/j.scs.2018.08.009>.
- [37] D. Lai, Z. Lian, W. Liu, C. Guo, W. Liu, K. Liu, Q. Chen, A comprehensive review of thermal comfort studies in urban open spaces, *Sci. Total Environ.* 742 (2020) 140092, <https://doi.org/10.1016/j.scitotenv.2020.140092>.
- [38] H. Holger Koss, On differences and similarities of applied wind comfort criteria, *J. Wind Eng. Ind. Aerod.* 94 (11) (2006) 781–797, <https://doi.org/10.1016/j.jweia.2006.06.005>.
- [39] Y. Peng, R. Buccolieri, Z. Gao, W. Ding, Indices employed for the assessment of “urban outdoor ventilation” - a review, *Atmos. Environ.* 223 (2020), <https://doi.org/10.1016/j.atmosenv.2019.117211>.
- [40] H. Sanaieian, M. Tenpierik, K.v.d. Linden, F. Mehdizadeh Seraj, S.M. Mofidi Shemrani, Review of the impact of urban block form on thermal performance, solar access and ventilation, *Renew. Sustain. Energy Rev.* 38 (2014) 551–560, <https://doi.org/10.1016/j.rser.2014.06.007>.
- [41] H. Akbari, D. Kolokotsa, Three decades of urban heat islands and mitigation technologies research, *Energy Build.* 133 (2016) 834–842, <https://doi.org/10.1016/j.enbuild.2016.09.067>.
- [42] D. Lai, W. Liu, T. Gan, K. Liu, Q. Chen, A review of mitigating strategies to improve the thermal environment and thermal comfort in urban outdoor spaces, *Sci. Total Environ.* 661 (2019) 337–353, <https://doi.org/10.1016/j.scitotenv.2019.01.062>.
- [43] Z. Yu, G. Yang, S. Zuo, G. Jørgensen, M. Koga, H. Vejre, Critical review on the cooling effect of urban blue-green space: a threshold-size perspective, *Urban For. Urban Green.* 49 (2020), <https://doi.org/10.1016/j.ufug.2020.126630>.
- [44] D. Mauree, E. Naboni, S. Coccolo, A.T.D. Perera, V.M. Nik, J.-L. Scarzezzini, A review of assessment methods for the urban environment and its energy sustainability to guarantee climate adaptation of future cities, *Renew. Sustain. Energy Rev.* 112 (2019) 733–746, <https://doi.org/10.1016/j.rser.2019.06.005>.
- [45] H. Bherwani, A. Singh, R. Kumar, Assessment methods of urban microclimate and its parameters: a critical review to take the research from lab to land, *Urban Clim.* 34 (2020), <https://doi.org/10.1016/j.uclim.2020.100690>.
- [46] P.A. Mirzaei, CFD modeling of micro and urban climates: problems to be solved in the new decade, *Sustain. Cities Soc.* 69 (2021), <https://doi.org/10.1016/j.scs.2021.102839>.
- [47] I. McRae, F. Freedman, A. Rivera, X. Li, J. Dou, I. Cruz, C. Ren, I. Dronova, H. Fraker, R. Bornstein, Integration of the WUDAPT, WRF, and ENVI-met models to simulate extreme daytime temperature mitigation strategies in San Jose, California, *Build. Environ.* 184 (2020), <https://doi.org/10.1016/j.enbuild.2020.107180>.
- [48] Z. Jandaghian, U. Berardi, Comparing urban canopy models for microclimate simulations in Weather Research and Forecasting Models, *Sustain. Cities Soc.* 55 (2020), <https://doi.org/10.1016/j.scs.2020.102025>.
- [49] P. Piroozmand, G. Mussetti, J. Allegretti, M.H. Mohammadi, E. Akrami, J. Carmeliet, Coupled CFD framework with mesoscale urban climate model: application to microscale urban flows with weak synoptic forcing, *J. Wind Eng. Ind. Aerod.* 197 (2020), <https://doi.org/10.1016/j.jweia.2019.104059>.
- [50] Y. Xuan, G. Yang, Q. Li, A. Mochida, Outdoor thermal environment for different urban forms under summer conditions, *Build. Simulat.* 9 (3) (2016) 281–296, <https://doi.org/10.1007/s12273-016-0274-7>.
- [51] H. Chen, R. Ooka, K. Harayama, S. Kato, X. Li, Study on outdoor thermal environment of apartment block in Shenzhen, China with coupled simulation of convection, radiation and conduction, *Energy Build.* 36 (12) (2004) 1247–1258, <https://doi.org/10.1016/j.enbuild.2003.07.003>.
- [52] Z. Liu, W. Cheng, C.Y. Jim, T.E. Morakinyo, Y. Shi, E. Ng, Heat mitigation benefits of urban green and blue infrastructures: a systematic review of modeling techniques, validation and scenario simulation in ENVI-met V4, *Build. Environ.* 200 (2021), <https://doi.org/10.1016/j.enbuild.2021.107939>.
- [53] C. Jacobs, L. Klok, M. Bruse, J. Cortesão, S. Lenzholzer, J. Kluck, Are urban water bodies really cooling? *Urban Clim.* 32 (2020) <https://doi.org/10.1016/j.uclim.2020.100607>.
- [54] M. Bruse, H. Fleer, Simulating surface-plant-air interactions inside urban environments with a three dimensional numerical model, *Environ. Model. Software* 13 (3–4) (1998) 373–384, [https://doi.org/10.1016/S1364-8152\(98\)00042-5](https://doi.org/10.1016/S1364-8152(98)00042-5).
- [55] T.E. Morakinyo, K.K.-L. Lau, C. Ren, E. Ng, Performance of Hong Kong's common trees species for outdoor temperature regulation, thermal comfort and energy saving, *Build. Environ.* 137 (2018) 157–170, <https://doi.org/10.1016/j.enbuild.2018.04.012>.
- [56] Ansys, Ansys Fluent-Fluid Simulation Software, 2021. <https://www.ansys.com/zh-cn/products/fluids/ansys-fluent>. (Accessed 15 October 2021).

- [57] CHAM, PHEONICS. <http://www.cham.co.uk/phoenics.php>, 2021. (Accessed 15 October 2021).
- [58] Cradle, scSTREAM. <https://www.cradle-cfd.com/product/scstream.html>, 2021. (Accessed 15 October 2021).
- [59] T.O. Foundation, OpenFOAM echnical guides. <https://openfoam.org/guides/>, 2021. (Accessed 9 January 2021).
- [60] ENVI-met, ENVI-met model architecture. <https://envi-met.info/doku.php?id=introduction:modelconcept>, 2021. (Accessed 1 September 2021).
- [61] W. Wang, T. Yang, Y. Li, Y. Xu, M. Chang, X. Wang, Identification of pedestrian-level ventilation corridors in downtown Beijing using large-eddy simulations, *Build. Environ.* 182 (2020), <https://doi.org/10.1016/j.buildenv.2020.107169>.
- [62] Y. Ashie, T. Kono, Urban-scale CFD analysis in support of a climate-sensitive design for the Tokyo Bay area, *Int. J. Climatol.* 31 (2) (2011) 174–188, <https://doi.org/10.1002/joc.2226>.
- [63] F. Chen, H. Kusaka, R. Bornstein, J. Ching, C.S.B. Grimmond, S. Grossman-Clarke, T. Loridan, K.W. Manning, A. Martilli, S. Miao, D. Sailor, F.P. Salamanca, H. Taha, M. Tewari, X. Wang, A.A. Wyszogrodzki, C. Zhang, The integrated WRF/urban modelling system: development, evaluation, and applications to urban environmental problems, *Int. J. Climatol.* 31 (2) (2011) 273–288, <https://doi.org/10.1002/joc.2158>.
- [64] B. Bueno, L. Norford, J. Hidalgo, G. Pigeon, The urban weather generator, *J. Build. Perform. Simulat.* 6 (4) (2012) 269–281, <https://doi.org/10.1080/19401493.2012.718797>.
- [65] A. Martilli, A. Clappier, M.W. Rotach, An urban surface exchange parameterisation for mesoscale models, *Boundary-Layer Meteorol.* 104 (2) (2002) 261–304, <https://doi.org/10.1023/A:1016099921195>.
- [66] D. Mauree, N. Blond, M. Kohler, A. Clappier, On the coherence in the boundary layer: development of a canopy interface model, *Front. Earth Sci.* 4 (2017), <https://doi.org/10.3389/feart.2016.00109>.
- [67] O. Brousse, A. Martilli, M. Foley, G. Mills, B. Bechtel, WUDAPT, an efficient land use producing data tool for mesoscale models? Integration of urban LCZ in WRF over Madrid, *Urban Clim.* 17 (2016) 116–134, <https://doi.org/10.1016/j.ulclim.2016.04.001>.
- [68] J. Ching, M. Brown, S. Burian, F. Chen, R. Cionco, A. Hanna, T. Hultgren, T. McPherson, D. Sailor, H. Taha, D. Williams, National urban database and access portal tool, *Bull. Am. Meteorol. Soc.* 90 (8) (2009) 1157–1168, <https://doi.org/10.1175/2009bams2675.1>.
- [69] C. Ren, M. Cai, X. Li, Y. Shi, L. See, Developing a rapid method for 3-dimensional urban morphology extraction using open-source data, *Sustain. Cities Soc.* 53 (2020), <https://doi.org/10.1016/j.scs.2019.101962>.
- [70] C. Wang, S. Wei, S. Du, D. Zhuang, Y. Li, X. Shi, X. Jin, X. Zhou, A systematic method to develop three dimensional geometry models of buildings for urban building energy modeling, *Sustain. Cities Soc.* 71 (2021), <https://doi.org/10.1016/j.scs.2021.102998>.
- [71] S. Zhu, S. Du, Y. Li, S. Wei, X. Jin, X. Zhou, X. Shi, A 3D spatiotemporal morphological database for urban green infrastructure and its applications, *Urban For. Urban Green.* 58 (2021), <https://doi.org/10.1016/j.ufug.2020.126935>.
- [72] W. Tao, Y. He, Recent advances in multiscale simulations of heat transfer and fluid flow problems, *Prog. Comput. Fluid Dynam. Int.* 9 (3–5) (2009) 150–157, <https://doi.org/10.1504/PCFD.2009.024813>.
- [73] Y.-L. He, W.-Q. Tao, Multiscale simulations of heat transfer and fluid flow problems, *J. Heat Tran.* 134 (3) (2012), <https://doi.org/10.1115/1.4005154>.
- [74] L. Tang, Y.K. Joshi, A multi-grid based multi-scale thermal analysis approach for combined mixed convection, conduction, and radiation due to discrete heating, *J. Heat Tran.* 127 (1) (2005) 18–26, <https://doi.org/10.1115/1.1852495>.
- [75] P.-Y. Cui, Y. Zhang, J.-H. Zhang, Y.-D. Huang, W.-Q. Tao, Application and numerical error analysis of multiscale method for air flow, heat and pollutant transfer through different scale urban areas, *Build. Environ.* 149 (2019) 349–365, <https://doi.org/10.1016/j.buildenv.2018.12.029>.
- [76] O. Temel, L. Bricteux, J. van Beeck, Coupled WRF-OpenFOAM study of wind flow over complex terrain, *J. Wind Eng. Ind. Aerod.* 174 (2018) 152–169, <https://doi.org/10.1016/j.jweia.2018.01.002>.
- [77] R. Kadaverugu, V. Purohit, C. Matli, R. Biniwale, Improving accuracy in simulation of urban wind flows by dynamic downscaling WRF with OpenFOAM, *Urban Clim.* 38 (2021), <https://doi.org/10.1016/j.ulclim.2021.100912>.
- [78] X. Yang, L. Zhao, M. Bruse, Q. Meng, An integrated simulation method for building energy performance assessment in urban environments, *Energy Build.* 54 (2012) 243–251, <https://doi.org/10.1016/j.enbuild.2012.07.042>.
- [79] S. Tsoka, T. Leduc, A. Rodler, Assessing the effects of urban street trees on building cooling energy needs: the role of foliage density and planting pattern, *Sustain. Cities Soc.* 65 (2021), <https://doi.org/10.1016/j.scs.2020.102633>.
- [80] M. Hadavi, H. Pasdarshahri, Impacts of urban buildings on microclimate and cooling systems efficiency: coupled CFD and BES simulations, *Sustain. Cities Soc.* 67 (2021), <https://doi.org/10.1016/j.scs.2021.102740>.
- [81] J. Franke, A. Hellsten, K.H. Schlünzen, B. Carissimo, The COST 732 Best Practice Guideline for CFD simulation of flows in the urban environment: a summary, *Int. J. Environ. Pollut.* 44 (1–4) (2011) 419–427, <https://doi.org/10.1504/IJEP.2011.038443>.
- [82] Y. Tominaga, A. Mochida, R. Yoshie, H. Kataoka, T. Nozu, M. Yoshikawa, T. Shirasawa, AJI guidelines for practical applications of CFD to pedestrian wind environment around buildings, *J. Wind Eng. Ind. Aerod.* 96 (10–11) (2008) 1749–1761, <https://doi.org/10.1016/j.jweia.2008.02.058>.
- [83] K. An, S.-M. Wong, J.C.-H. Fung, E. Ng, Revisit of prevailing practice guidelines and investigation of topographical treatment techniques in CFD-Based air ventilation assessments, *Build. Environ.* 169 (2020), <https://doi.org/10.1016/j.buildenv.2019.106580>.
- [84] Z. Tong, Y. Chen, A. Malkawi, Defining the Influence Region in neighborhood-scale CFD simulations for natural ventilation design, *Appl. Energy* 182 (2016) 625–633, <https://doi.org/10.1016/j.apenergy.2016.08.098>.
- [85] A. Forouzandeh, Numerical modeling validation for the microclimate thermal condition of semi-closed courtyard spaces between buildings, *Sustain. Cities Soc.* 36 (2018) 327–345, <https://doi.org/10.1016/j.scs.2017.07.025>.
- [86] F. Salata, I. Golasi, R. de Lieto Vollaro, A. de Lieto Vollaro, Urban microclimate and outdoor thermal comfort. A proper procedure to fit ENVI-met simulation outputs to experimental data, *Sustain. Cities Soc.* 26 (2016) 318–343, <https://doi.org/10.1016/j.scs.2016.07.005>.
- [87] A. Middel, K. Häb, A.J. Brazel, C.A. Martin, S. Guhathakurta, Impact of urban form and design on mid-afternoon microclimate in Phoenix Local Climate Zones, *Landsct. Urban Plann.* 122 (2014) 16–28, <https://doi.org/10.1016/j.landurbplan.2013.11.004>.
- [88] J.-Y. Deng, N.H. Wong, Impact of urban canyon geometries on outdoor thermal comfort in central business districts, *Sustain. Cities Soc.* 53 (2020), <https://doi.org/10.1016/j.scs.2019.101966>.
- [89] A. Zhang, R. Bokel, A. van den Dobbelsteen, Y. Sun, Q. Huang, Q. Zhang, An integrated school and schoolyard design method for summer thermal comfort and energy efficiency in Northern China, *Build. Environ.* 124 (2017) 369–387, <https://doi.org/10.1016/j.buildenv.2017.08.024>.
- [90] ENVI-met, Timesteps section. [https://envi-met.info/doku.php?id=timesteps&\[\]=time&s\[\]=step](https://envi-met.info/doku.php?id=timesteps&[]=time&s[]=step), 2017. (Accessed 1 September 2021).
- [91] ENVI-met, Timing section. [https://envi-met.info/doku.php?id=timing&s\[\]=update&s\[\]=interval](https://envi-met.info/doku.php?id=timing&s[]=update&s[]=interval), 2017. (Accessed 1 September 2021).
- [92] A. Ricci, I. Kalkman, B. Blocken, M. Burlando, A. Freda, M.P. Repetto, Local-scale forcing effects on wind flows in an urban environment: impact of geometrical simplifications, *J. Wind Eng. Ind. Aerod.* 170 (2017) 238–255, <https://doi.org/10.1016/j.jweia.2017.08.001>.
- [93] W.C. Skamarock, J.B. Klemp, J. Dudhia, D.O. Gill, Z. Liu, J. Berner, J. Berner, W. Wang, J. Powers, M. Duda, D. Barker, X. Huang, A Description of the Advanced Research WRF Model, 2021, <https://doi.org/10.5065/1dfh-6p97>, Version 4.3.
- [94] M.M.F. Wong, J.C.H. Fung, J. Ching, P.P.S. Yeung, J.W.P. Tse, C. Ren, R. Wang, M. Cai, Evaluation of uWRF performance and modeling guidance based on WUDAPT and NUDAPT UCP datasets for Hong Kong, *Urban Clim.* 28 (2019), <https://doi.org/10.1016/j.ulclim.2019.100460>.
- [95] X. Zhang, G.-J. Steeneveld, D. Zhou, R.J. Ronda, C. Duan, S. Koopmans, A.A. M. Holtslag, Modelling urban meteorology with increasing refinements for the complex morphology of a typical Chinese city (Xi'an), *Build. Environ.* 182 (2020), <https://doi.org/10.1016/j.buildenv.2020.107109>.
- [96] R. Wang, C. Ren, Y. Xu, K.K.-L. Lau, Y. Shi, Mapping the local climate zones of urban areas by GIS-based and WUDAPT methods: a case study of Hong Kong, *Urban Clim.* 24 (2018) 567–576, <https://doi.org/10.1016/j.ulclim.2017.10.001>.
- [97] I.D. Stewart, T.R. Oke, E.S. Krayenhoff, Evaluation of the 'local climate zone' scheme using temperature observations and model simulations, *Int. J. Climatol.* 34 (4) (2014) 1062–1080, <https://doi.org/10.1002/joc.3746>.
- [98] Q. Zhang, D. Xu, D. Zhou, Y. Yang, A. Rogora, Associations between urban thermal environment and physical indicators based on meteorological data in Foshan City, *Sustain. Cities Soc.* 60 (2020), <https://doi.org/10.1016/j.scs.2020.102288>.
- [99] M. Taleghani, L. Kleerekoper, M. Tenpierik, A. van den Dobbelsteen, Outdoor thermal comfort within five different urban forms in The Netherlands, *Build. Environ.* 83 (2015) 65–78, <https://doi.org/10.1016/j.buildenv.2014.03.014>.
- [100] I.D. Stewart, T.R. Oke, Local climate zones for urban temperature studies, *Bull. Am. Meteorol. Soc.* 93 (2012) 1879–1900, <https://doi.org/10.1175/BAMS-D-i>.
- [101] X. Yang, L. Yao, T. Jin, L.L.H. Peng, Z. Jiang, Z. Hu, Y. Ye, Assessing the thermal behavior of different local climate zones in the Nanjing metropolis, China, *Build. Environ.* 137 (2018) 171–184, <https://doi.org/10.1016/j.buildenv.2018.04.009>.
- [102] X. Yang, Y. Li, Z. Luo, P.W. Chan, The urban cool island phenomenon in a high-rise high-density city and its mechanisms, *Int. J. Climatol.* 37 (2) (2017) 890–904, <https://doi.org/10.1002/joc.4747>.
- [103] P. Höppe, The physiological equivalent temperature - a universal index for the biometeorological assessment of the thermal environment, *Int. J. Biometeorol.* 43 (1999) 71–75, <https://doi.org/10.1007/s004840050118>.
- [104] A.P. Gagge, A.J.A. Stolwijk, Y. Nishi, An effective temperature scale based on a simple model of human physiological regulatory response, *Build. Eng.* 77 (1) (1971) 247–262. <http://hdl.handle.net/2115/37901>.
- [105] J. Pickup, R. De Daer, An outdoor thermal comfort index (OUT_SET*) - Part I - the model and its assumptions, in: 5th International Congress of Biometeorology and International Conference on Urban Climatology, Sydney, Australia, 1999.
- [106] D. Fiala, G. Havenith, P. Brode, B. Kampmann, G. Jendritzky, UTCI-Fiala multi-node model of human heat transfer and temperature regulation, *Int. J. Biometeorol.* 56 (3) (2012) 429–441, <https://doi.org/10.1007/s00484-011-0424-7>.
- [107] P. Höppe, Heat balance modelling, *Experientia* 49 (1993) 741–746, <https://doi.org/10.1007/BF01923542>.
- [108] Z. Fang, X. Feng, J. Liu, Z. Lin, C.M. Mak, J. Niu, K.-T. Tse, X. Xu, Investigation into the differences among several outdoor thermal comfort indices against field survey in subtropics, *Sustain. Cities Soc.* 44 (2019) 676–690, <https://doi.org/10.1016/j.scs.2018.10.022>.
- [109] P. Brode, D. Fiala, K. Blazejczyk, I. Holmer, G. Jendritzky, B. Kampmann, B. Tin, G. Havenith, Deriving the operational procedure for the universal thermal climate index (UTCI), *Int. J. Biometeorol.* 56 (3) (2012) 481–494, <https://doi.org/10.1007/s00484-011-0454-1>.

- [110] P.O. Fanger, Thermal Comfort. Analysis and Applications in Environmental Engineering, 1970, p. 244.
- [111] R.D. Brown, T.J. Gillespie, Estimating outdoor thermal comfort using a cylindrical radiation thermometer and an energy budget model, *Int. J. Biometeorol.* 30 (1) (1986) 43–52, <https://doi.org/10.1007/BF02192058>.
- [112] B. Givoni, Estimation of the Effect of Climate on Man: Development of a New Thermal Index, Technion-Israel Institute of Technology, Haifa, 1963.
- [113] G. Jendritzky, W. Nübler, A model analyzing the urban thermal environment in physiologically significant terms, *Arch. Meteorol. Geophys. Bioclimatol. Ser. B* 29 (1981), <https://doi.org/10.1007/BF02263308>.
- [114] N.A. Kenny, J.S. Warland, R.D. Brown, T.G. Gillespie, Part A: assessing the performance of the COMFA outdoor thermal comfort model on subjects performing physical activity, *Int. J. Biometeorol.* 53 (5) (2009) 415–428, <https://doi.org/10.1007/s00484-009-0226-3>.
- [115] N.A. Kenny, J.S. Warland, R.D. Brown, T.G. Gillespie, Part B: revisions to the COMFA outdoor thermal comfort model for application to subjects performing physical activity, *Int. J. Biometeorol.* 53 (5) (2009) 429–441, <https://doi.org/10.1007/s00484-009-0227-2>.
- [116] A. Angelotti, V. Dessimoz, G. Scudo, The Evaluation of Thermal Comfort Conditions in Simplified Urban Spaces: the COMFA+ Model 2nd PALENC Conference and 28th AIVC Conference on Building Low Energy Cooling and Advanced Ventilation Technologies in the 21st Century, Crete island, Greece, 2007.
- [117] D. Pearlmutter, P. Berliner, E. Shaviv, Integrated modeling of pedestrian energy exchange and thermal comfort in urban street canyons, *Build. Environ.* 42 (6) (2007) 2396–2409, <https://doi.org/10.1016/j.buildenv.2006.06.006>.
- [118] M. Nikolopoulou, N. Baker, K. Steemers, Thermal comfort in outdoor urban spaces understanding the human parameter, *Sol. Energy* 70 (2001) 227–235, [https://doi.org/10.1016/S0038-092X\(00\)00093-1](https://doi.org/10.1016/S0038-092X(00)00093-1).
- [119] D. Lai, D. Guo, Y. Hou, C. Lin, Q. Chen, Studies of outdoor thermal comfort in northern China, *Build. Environ.* 77 (2014) 110–118, <https://doi.org/10.1016/j.buildenv.2014.03.026>.
- [120] K. Blazejczyk, Y. Epstein, G. Jendritzky, H. Staiger, B. Tinz, Comparison of UTCI to selected thermal indices, *Int. J. Biometeorol.* 56 (3) (2012) 515–535, <https://doi.org/10.1007/s00484-011-0453-2>.
- [121] Z. Lian, B. Liu, R.D. Brown, Exploring the suitable assessment method and best performance of human energy budget models for outdoor thermal comfort in hot and humid climate area, *Sustain. Cities Soc.* 63 (2020), <https://doi.org/10.1016/j.scs.2020.102423>.
- [122] M.A. Ruiz, E.N. Correa, Suitability of different comfort indices for the prediction of thermal conditions in tree-covered outdoor spaces in arid cities, *Theor. Appl. Climatol.* 122 (1–2) (2014) 69–83, <https://doi.org/10.1007/s00704-014-1279-8>.
- [123] J.C.R. Hunt, E.C. Poulton, J.C. Mumford, The effects of wind on people; new criteria based on wind tunnel experiments, *Build. Environ.* 11 (1) (1976) 15–28, [https://doi.org/10.1016/0360-1323\(76\)90015-9](https://doi.org/10.1016/0360-1323(76)90015-9).
- [124] W.H. Melbourne, Criteria for environmental wind conditions, *J. Ind. Aerod.* 3 (1978) 241–249, [https://doi.org/10.1016/0167-6105\(78\)90013-2](https://doi.org/10.1016/0167-6105(78)90013-2).
- [125] T.V. Lawson, A.D. Penwarden, The Effects of Wind on People in the Vicinity of Buildings, Proceedings of the Fourth International Conference on Wind Effects on Buildings and Structures, Cambridge University Press, Heathrow, 1975, pp. 605–622.
- [126] N. Ilyumov, A.G. Davenport, The ground level wind environment in built-up areas, in: Proceedings of the Fourth International Conference on Wind Effects on Buildings and Structures, Cambridge University Press, Heathrow, 1975, pp. 403–422.
- [127] M.J. Soligo, P.A. Irwin, C.J. Williams, G.D. Schuyler, A comprehensive assessment of pedestrian comfort including thermal effects, *J. Wind Eng. Ind. Aerod.* 77 (1998) 753–766, [https://doi.org/10.1016/S0167-6105\(98\)00189-5](https://doi.org/10.1016/S0167-6105(98)00189-5).
- [128] Y. Du, C.M. Mak, K. Kwok, K.-T. Tse, T.-c. Lee, Z. Ai, J. Liu, J. Niu, New criteria for assessing low wind environment at pedestrian level in Hong Kong, *Build. Environ.* 123 (2017) 23–36, <https://doi.org/10.1016/j.buildenv.2017.06.036>.
- [129] X. Shi, Y. Zhu, J. Duan, R. Shao, J. Wang, Assessment of pedestrian wind environment in urban planning design, *Landscape. Urban Plann.* 140 (2015) 17–28, <https://doi.org/10.1016/j.landurbplan.2015.03.013>.
- [130] E. Ng, V. Cheng, Urban human thermal comfort in hot and humid Hong Kong, *Energy Build.* 55 (2012) 51–65, <https://doi.org/10.1016/j.enbuild.2011.09.025>.
- [131] B. Blocken, J. Carmeliet, Pedestrian wind environment around buildings: literature review and practical examples, *J. Therm. Envelope Build. Sci.* 28 (2) (2004) 107–159, <https://doi.org/10.1177/1097196304044396>.
- [132] S.H.L. Yim, J.C.H. Fung, A.K.H. Lau, S.C. Kot, Air ventilation impacts of the “wall effect” resulting from the alignment of high-rise buildings, *Atmos. Environ.* 43 (32) (2009) 4982–4994, <https://doi.org/10.1016/j.atmosenv.2009.07.002>.
- [133] D. Hamlyn, R. Britter, A numerical study of the flow field and exchange processes within a canopy of urban-type roughness, *Atmos. Environ.* 39 (18) (2005) 3243–3254, <https://doi.org/10.1016/j.atmosenv.2005.02.020>.
- [134] I. Panagiotou, M.K. Neophytou, D. Hamlyn, R.E. Britter, City breathability as quantified by the exchange velocity and its spatial variation in real inhomogeneous urban geometries: an example from central London urban area, *Sci. Total Environ.* 442 (2013) 466–477, <https://doi.org/10.1016/j.scitotenv.2012.09.001>.
- [135] C. Liu, D. Leung, M. Barth, On the prediction of air and pollutant exchange rates in street canyons of different aspect ratios using large-eddy simulation, *Atmos. Environ.* (2005), <https://doi.org/10.1016/j.atmosenv.2004.08.036>.
- [136] Y.-K. Ho, C.-H. Liu, Street-level ventilation in hypothetical urban areas, *Atmosphere* 8 (12) (2017), <https://doi.org/10.3390/atmos8070124>.
- [137] X. Li, C. Liu, D. Leung, Development of a k- ϵ model for the determination of air exchange rates for street canyons, *Atmos. Environ.* 39 (38) (2005) 7285–7296, <https://doi.org/10.1016/j.atmosenv.2005.09.007>.
- [138] J. Hang, M. Sandberg, Y. Li, Age of air and air exchange efficiency in idealized city models, *Build. Environ.* 44 (8) (2009) 1714–1723, <https://doi.org/10.1016/j.buildenv.2008.11.013>.
- [139] J. Hang, Y. Li, M. Sandberg, R. Buccolieri, S. Di Sabatino, The influence of building height variability on pollutant dispersion and pedestrian ventilation in idealized high-rise urban areas, *Build. Environ.* 56 (2012) 346–360, <https://doi.org/10.1016/j.buildenv.2012.03.023>.
- [140] J. Hang, Q. Wang, X. Chen, M. Sandberg, W. Zhu, R. Buccolieri, S. Di Sabatino, City breathability in medium density urban-like geometries evaluated through the pollutant transport rate and the net escape velocity, *Build. Environ.* 94 (2015) 166–182, <https://doi.org/10.1016/j.buildenv.2015.08.002>.
- [141] M. Bady, S. Kato, H. Huang, Towards the application of indoor ventilation efficiency indices to evaluate the air quality of urban areas, *Build. Environ.* 43 (12) (2008) 1991–2004, <https://doi.org/10.1016/j.buildenv.2007.11.013>.
- [142] M. Sandberg, M. Sjöberg, The use of moments for assessing air quality in ventilated rooms, *Build. Environ.* 18 (4) (1983) 181–197, [https://doi.org/10.1016/0360-1323\(83\)90026-4](https://doi.org/10.1016/0360-1323(83)90026-4).
- [143] N. Antoniou, H. Montazeri, H. Wigo, M.K.A. Neophytou, B. Blocken, M. Sandberg, CFD and wind-tunnel analysis of outdoor ventilation in a real compact heterogeneous urban area: evaluation using “air delay”, *Build. Environ.* 126 (2017) 355–372, <https://doi.org/10.1016/j.buildenv.2017.10.013>.
- [144] R. Giridharan, S.S.Y. Lau, S. Ganeshan, Nocturnal heat island effect in urban residential developments of Hong Kong, *Energy Build.* 37 (9) (2005) 964–971, <https://doi.org/10.1016/j.enbuild.2004.12.005>.
- [145] N. Nazarian, J.A. Acero, L. Norford, Outdoor thermal comfort autonomy: performance metrics for climate-conscious urban design, *Build. Environ.* 155 (2019) 145–160, <https://doi.org/10.1016/j.buildenv.2019.03.028>.
- [146] S. Yin, W. Lang, Y. Xiao, The synergistic effect of street canyons and neighbourhood layout design on pedestrian-level thermal comfort in hot-humid area of China, *Sustain. Cities Soc.* 49 (2019), <https://doi.org/10.1016/j.scs.2019.101571>.
- [147] A. Chatzidimitriou, S. Yannas, Street canyon design and improvement potential for urban open spaces; the influence of canyon aspect ratio and orientation on microclimate and outdoor comfort, *Sustain. Cities Soc.* 33 (2017) 85–101, <https://doi.org/10.1016/j.scs.2017.05.019>.
- [148] B. He, L. Ding, D. Prasad, Wind-sensitive urban planning and design: precinct ventilation performance and its potential for local warming mitigation in an open midrise gridiron precinct, *J. Build. Eng.* 29 (2020), <https://doi.org/10.1016/j.jobe.2019.101145>.
- [149] B. He, L. Ding, D. Prasad, Relationships among local-scale urban morphology, urban ventilation, urban heat island and outdoor thermal comfort under sea breeze influence, *Sustain. Cities Soc.* 60 (2020), <https://doi.org/10.1016/j.scs.2020.102289>.
- [150] O.M. Galal, D.J. Sailor, H. Mahmoud, The impact of urban form on outdoor thermal comfort in hot arid environments during daylight hours, case study: new Aswan, *Build. Environ.* 184 (2020), <https://doi.org/10.1016/j.buildenv.2020.107222>.
- [151] D. Xu, D. Zhou, Y. Wang, X. Meng, W. Chen, Y. Yang, Temporal and spatial variations of urban climate and derivation of an urban climate map for Xi'an, China, *Sustain. Cities Soc.* 52 (2020), <https://doi.org/10.1016/j.scs.2019.101850>.
- [152] A. Azhdari, A. Soltani, M. Alidadi, Urban morphology and landscape structure effect on land surface temperature: evidence from Shiraz, a semi-arid city, *Sustain. Cities Soc.* 41 (2018) 853–864, <https://doi.org/10.1016/j.scs.2018.06.034>.
- [153] M. Unal Cilek, A. Cilek, Analyses of land surface temperature (LST) variability among local climate zones (LCZs) comparing Landsat-8 and ENVI-met model data, *Sustain. Cities Soc.* 69 (2021), <https://doi.org/10.1016/j.scs.2021.102877>.
- [154] G. Guo, X. Zhou, Z. Wu, R. Xiao, Y. Chen, Characterizing the impact of urban morphology heterogeneity on land surface temperature in Guangzhou, China, *Environ. Model. Software* 84 (2016) 427–439, <https://doi.org/10.1016/j.envsoft.2016.06.021>.
- [155] T. Houet, G. Pigeon, Mapping urban climate zones and quantifying climate behaviors—an application on Toulouse urban area (France), *Environ. Pollut.* 159 (8–9) (2011) 2180–2192, <https://doi.org/10.1016/j.envpol.2010.12.027>.
- [156] K.K.-L. Lau, S.C. Chung, C. Ren, Outdoor thermal comfort in different urban settings of sub-tropical high-density cities: an approach of adopting local climate zone (LCZ) classification, *Build. Environ.* 154 (2019) 227–238, <https://doi.org/10.1016/j.buildenv.2019.03.005>.
- [157] J. Ngarambe, J.W. Oh, M.A. Su, M. Santamouris, G.Y. Yun, Influences of wind speed, sky conditions, land use and land cover characteristics on the magnitude of the urban heat island in Seoul: an exploratory analysis, *Sustain. Cities Soc.* 71 (2021), <https://doi.org/10.1016/j.scs.2021.102953>.
- [158] Y. Sasaki, K. Matsuo, M. Yokoyama, M. Sasaki, T. Tanaka, S. Sadohara, Sea breeze effect mapping for mitigating summer urban warming: for making urban environmental climate map of Yokohama and its surrounding area, *Urban Clim.* 24 (2018) 529–550, <https://doi.org/10.1016/j.uclim.2017.07.003>.
- [159] H. Du, W. Cai, Y. Xu, Z. Wang, Y. Wang, Y. Cai, Quantifying the cool island effects of urban green spaces using remote sensing Data, *Urban For. Urban Green.* 27 (2017) 24–31, <https://doi.org/10.1016/j.ufug.2017.06.008>.
- [160] X. Sun, X. Tan, K. Chen, S. Song, X. Zhu, D. Hou, Quantifying Landscape-Metrics Impacts on Urban Green-Spaces and Water-Bodies Cooling Effect: the Study of

- Nanjing, China, vol. 55, *Urban Forestry & Urban Greening*, 2020, <https://doi.org/10.1016/j.ufug.2020.126838>.
- [161] Z. Yu, X. Guo, G. Jørgensen, H. Vejre, How can urban green spaces be planned for climate adaptation in subtropical cities? *Ecol. Indicat.* 82 (2017) 152–162, <https://doi.org/10.1016/j.ecolind.2017.07.002>.
- [162] Z. Qiao, X. Xu, F. Wu, W. Luo, F. Wang, L. Liu, Z. Sun, Urban ventilation network model: a case study of the core zone of capital function in Beijing metropolitan area, *J. Clean. Prod.* 168 (2017) 526–535, <https://doi.org/10.1016/j.jclepro.2017.09.006>.
- [163] E. Johansson, Influence of urban geometry on outdoor thermal comfort in a hot dry climate: a study in Fez, Morocco, *Build. Environ.* 41 (10) (2006) 1326–1338, <https://doi.org/10.1016/j.buildenv.2005.05.022>.
- [164] R. Emmanuel, E. Johansson, Influence of urban morphology and sea breeze on hot humid microclimate: the case of Colombo, Sri Lanka, *Clim. Res.* 30 (2006) 189–200, <https://doi.org/10.3354/cr030189>.
- [165] A.N. Kakon, N. Mishima, S. Kojima, Simulation of the urban thermal comfort in a high density tropical city: analysis of the proposed urban construction rules for Dhaka, Bangladesh, *Build. Simulat.* 2 (4) (2009), <https://doi.org/10.1007/s12273-009-9321-y>.
- [166] E. Andreou, Thermal comfort in outdoor spaces and urban canyon microclimate, *Renew. Energy* 55 (2013) 182–188, <https://doi.org/10.1016/j.renene.2012.12.040>.
- [167] F. Ali-Toudert, H. Mayer, Numerical study on the effects of aspect ratio and orientation of an urban street canyon on outdoor thermal comfort in hot and dry climate, *Build. Environ.* 41 (2) (2006) 94–108, <https://doi.org/10.1016/j.buildenv.2005.01.013>.
- [168] R. Emmanuel, H. Rosenlund, E. Johansson, Urban shading-a design option for the tropics? A study in Colombo, Sri Lanka, *Int. J. Climatol.* 27 (14) (2007) 1995–2004, <https://doi.org/10.1002/joc.1609>.
- [169] T.R. Oke, Street design and urban canopy layer climate, *Energy Build.* 11 (1988) 103–113, [https://doi.org/10.1016/0378-7788\(88\)90026-6](https://doi.org/10.1016/0378-7788(88)90026-6).
- [170] M.W. Yahia, E. Johansson, Influence of urban planning regulations on the microclimate in a hot dry climate: the example of Damascus, Syria, *J. Hous. Built Environ.* 28 (1) (2013) 51–65, <https://doi.org/10.1007/s10901-012-9280-y>.
- [171] P. Lin, Z. Gou, S. Lau, H. Qin, The impact of urban design descriptors on outdoor thermal environment: a literature review, *Energies* 10 (12) (2017), <https://doi.org/10.3390/en10122151>.
- [172] M.K. Svensson, Sky view factor analysis – implications for urban air temperature differences, *Meteorol. Appl.* 11 (3) (2004) 201–211, <https://doi.org/10.1017/s1350482704001288>.
- [173] J. Unger, Intra-urban relationship between surface geometry and urban heat island: review and new approach, *Clim. Res.* 27 (2004) 253–264, <https://doi.org/10.3354/cr027253>.
- [174] M.W. Rotach, On the influence of the urban roughness sublayer on turbulence and dispersion, *Atmos. Environ.* 33 (1999) 4001–4008, [https://doi.org/10.1016/S1352-2310\(99\)00141-7](https://doi.org/10.1016/S1352-2310(99)00141-7).
- [175] Y. Xu, C. Ren, P. Ma, J. Ho, W. Wang, K.K.-L. Lau, H. Lin, E. Ng, Urban morphology detection and computation for urban climate research, *Landsc. Urban Plann.* 167 (2017) 212–224, <https://doi.org/10.1016/j.landurbplan.2017.06.018>.
- [176] K. Giannopoulou, M. Santamouris, I. Livada, C. Georgakis, Y. Caouris, The impact of canyon geometry on intra urban and urban: suburban night temperature differences under warm weather conditions, *Pure Appl. Geophys.* 167 (11) (2010) 1433–1449, <https://doi.org/10.1007/s00024-010-0099-8>.
- [177] C. Yuan, L. Chen, Mitigating urban heat island effects in high-density cities based on sky view factor and urban morphological understanding: a study of Hong Kong, *Architect. Sci. Rev.* 54 (4) (2011) 305–315, <https://doi.org/10.1080/0038628.2011.613644>.
- [178] T. Gál, J. Unger, Detection of ventilation paths using high-resolution roughness parameter mapping in a large urban area, *Build. Environ.* 44 (1) (2009) 198–206, <https://doi.org/10.1016/j.buildenv.2008.02.008>.
- [179] L. Grunwald, M. Kossmann, S. Weber, Mapping urban cold-air paths in a Central European city using numerical modelling and geospatial analysis, *Urban Clim.* 29 (2019), <https://doi.org/10.1016/j.uclim.2019.100503>.
- [180] L. Grunwald, A.-K. Schneider, B. Schröder, S. Weber, Predicting urban cold-air paths using boosted regression trees, *Landsc. Urban Plann.* 201 (2020), <https://doi.org/10.1016/j.landurbplan.2020.103843>.
- [181] A.B. Barlag, W. Kuttler, The significance of country breezes for urban planning, *Energy Build.* 15 (3–4) (1990) 291–297, [https://doi.org/10.1016/0378-7788\(90\)90001-Y](https://doi.org/10.1016/0378-7788(90)90001-Y).
- [182] H. Mayer, W. Beckroge, A. Matzarakis, Bestimmung von stadt-klimarelevanten Luftleitbahnen, UVP report, 1994, pp. 265–268.
- [183] M.H. Amaral, L.L. Benites-Lazaro, P. Antonio de Almeida Sinisgalli, H. Prates da Fonseca Alves, L.L. Giatti, Environmental injustices on green and blue infrastructure: urban nexus in a macrometropolitan territory, *J. Clean. Prod.* 289 (2021), <https://doi.org/10.1016/j.jclepro.2021.125829>.
- [184] H. Lee, H. Mayer, L. Chen, Contribution of trees and grasslands to the mitigation of human heat stress in a residential district of Freiburg, Southwest Germany, *Landsc. Urban Plann.* 148 (2016) 37–50, <https://doi.org/10.1016/j.landurbplan.2015.12.004>.
- [185] A. Chatzidimitriou, S. Yannas, Microclimate development in open urban spaces: the influence of form and materials, *Energy Build.* 108 (2015) 156–174, <https://doi.org/10.1016/j.enbuild.2015.08.048>.
- [186] F. Yang, S.S.Y. Lau, F. Qian, Thermal comfort effects of urban design strategies in high-rise urban environments in a sub-tropical climate, *Architect. Sci. Rev.* 54 (4) (2011) 285–304, <https://doi.org/10.1080/0038628.2011.613646>.
- [187] E. Ng, L. Chen, Y. Wang, C. Yuan, A study on the cooling effects of greening in a high-density city: an experience from Hong Kong, *Build. Environ.* 47 (2012) 256–271, <https://doi.org/10.1016/j.buildenv.2011.07.014>.
- [188] T.E. Morakinyo, W. Ouyang, K.K. Lau, C. Ren, E. Ng, Right tree, right place (urban canyon): tree species selection approach for optimum urban heat mitigation - development and evaluation, *Sci. Total Environ.* 719 (2020) 137461, <https://doi.org/10.1016/j.scitotenv.2020.137461>.
- [189] B.A. Norton, A.M. Coutts, S.J. Livesley, R.J. Harris, A.M. Hunter, N.S.G. Williams, Planning for cooler cities: a framework to prioritise green infrastructure to mitigate high temperatures in urban landscapes, *Landsc. Urban Plann.* 134 (2015) 127–138, <https://doi.org/10.1016/j.landurbplan.2014.10.018>.
- [190] D.D. Milošević, I.V. Bajšanski, S.M. Savić, Influence of changing trees locations on thermal comfort on street parking lot and footways, *Urban For. Urban Green.* 23 (2017) 113–124, <https://doi.org/10.1016/j.ufug.2017.03.011>.
- [191] L. Kong, K.K.-L. Lau, C. Yuan, Y. Chen, Y. Xu, C. Ren, E. Ng, Regulation of outdoor thermal comfort by trees in Hong Kong, *Sustain. Cities Soc.* 31 (2017) 12–25, <https://doi.org/10.1016/j.scs.2017.01.018>.
- [192] M.F. Shahidan, M.K.M. Shariff, P. Jones, E. Salleh, A.M. Abdullah, A comparison of Mesua ferrea L. and Hura crepitans L. for shade creation and radiation modification in improving thermal comfort, *Landsc. Urban Plann.* 97 (3) (2010) 168–181, <https://doi.org/10.1016/j.landurbplan.2010.05.008>.
- [193] T.E. Morakinyo, K.W.D.K.C. Dahanayake, O.B. Adegun, A.A. Balogun, Modelling the effect of tree-shading on summer indoor and outdoor thermal condition of two similar buildings in a Nigerian university, *Energy Build.* 130 (2016) 721–732, <https://doi.org/10.1016/j.enbuild.2016.08.087>.
- [194] S. Oliveira, H. Andrade, T. Vaz, The cooling effect of green spaces as a contribution to the mitigation of urban heat: a case study in Lisbon, *Build. Environ.* 46 (11) (2011) 2186–2194, <https://doi.org/10.1016/j.buildenv.2011.04.034>.
- [195] Z. Chen, L. Zhao, Q. Meng, C. Wang, Y. Zhai, F. Wang, Field measurements on microclimate in residential community in Guangzhou, China, *Front. Architect. Civ. Eng. China* 3 (4) (2009) 462–468, <https://doi.org/10.1007/s11709-009-0066-6>.
- [196] H. Du, X. Song, H. Jiang, Z. Kan, Z. Wang, Y. Cai, Research on the cooling island effects of water body: a case study of Shanghai, China, *Ecol. Indicat.* 67 (2016) 31–38, <https://doi.org/10.1016/j.ecolind.2016.02.040>.
- [197] E.A. Hathway, S. Sharples, The interaction of rivers and urban form in mitigating the Urban Heat Island effect: a UK case study, *Build. Environ.* 58 (2012) 14–22, <https://doi.org/10.1016/j.buildenv.2012.06.013>.
- [198] S. Hamada, T. Ohta, Seasonal variations in the cooling effect of urban green areas on surrounding urban areas, *Urban For. Urban Green.* 9 (1) (2010) 15–24, <https://doi.org/10.1016/j.ufug.2009.10.002>.
- [199] F. Kong, H. Yin, C. Wang, G. Cavan, P. James, A satellite image-based analysis of factors contributing to the green-space cool island intensity on a city scale, *Urban For. Urban Green.* 13 (4) (2014) 846–853, <https://doi.org/10.1016/j.ufug.2014.09.009>.
- [200] R.C. Estoque, Y. Murayama, S.W. Myint, Effects of landscape composition and pattern on land surface temperature: an urban heat island study in the megacities of Southeast Asia, *Sci. Total Environ.* 577 (2017) 349–359, <https://doi.org/10.1016/j.scitotenv.2016.10.195>.
- [201] M. Maimaitiyiming, A. Ghulam, T. Tiyp, F. Pla, P. Latorre-Carmona, Ü. Halik, M. Sawut, M. Caetano, Effects of green space spatial pattern on land surface temperature: implications for sustainable urban planning and climate change adaptation, *ISPRS J. Photogrammetry Remote Sens.* 89 (2014) 59–66, <https://doi.org/10.1016/j.isprsjprs.2013.12.010>.
- [202] N.E. Theeuwes, A. Solcerová, G.J. Steeneveld, Modeling the influence of open water surfaces on the summertime temperature and thermal comfort in the city, *J. Geophys. Res. Atmos.* 118 (16) (2013) 8881–8896, <https://doi.org/10.1002/jgrd.50704>.
- [203] R. Sun, L. Chen, How can urban water bodies be designed for climate adaptation? *Landsc. Urban Plann.* 105 (1–2) (2012) 27–33, <https://doi.org/10.1016/j.landurbplan.2011.11.018>.
- [204] C.R. Chang, M.-H. Li, S.-D. Chang, A preliminary study on the local cool-island intensity of Taipei city parks, *Landsc. Urban Plann.* 80 (4) (2007) 386–395, <https://doi.org/10.1016/j.landurbplan.2006.09.005>.
- [205] G. Yang, Z. Yu, G. Jørgensen, H. Vejre, How can urban blue-green space be planned for climate adaption in high-latitude cities? seasonal Perspect. Sustain. Cities Soc. 53 (2020) <https://doi.org/10.1016/j.scs.2019.101932>.
- [206] H. Fan, Z. Yu, G. Yang, T.Y. Liu, T.Y. Liu, C.H. Hung, H. Vejre, How to cool hot-humid (Asian) cities with urban trees? An optimal landscape size perspective, *Agric. For. Meteorol.* 265 (2019) 338–348, <https://doi.org/10.1016/j.agrformet.2018.11.027>.
- [207] J. Peng, P. Xie, Y. Liu, J. Ma, Urban thermal environment dynamics and associated landscape pattern factors: a case study in the Beijing metropolitan region, *Remote Sens. Environ.* 173 (2016) 145–155, <https://doi.org/10.1016/j.rse.2015.11.027>.
- [208] X. Cao, A. Onishi, J. Chen, H. Imura, Quantifying the cool island intensity of urban parks using ASTER and IKONOS data, *Landsc. Urban Plann.* 96 (4) (2010) 224–231, <https://doi.org/10.1016/j.landurbplan.2010.03.008>.
- [209] M. Vaz Monteiro, K.J. Doick, P. Handley, A. Peace, The impact of greenspace size on the extent of local nocturnal air temperature cooling in London, *Urban For. Urban Green.* 16 (2016) 160–169, <https://doi.org/10.1016/j.ufug.2016.02.008>.
- [210] W. Kuang, Y. Liu, Y. Dou, W. Chi, G. Chen, C. Gao, T. Yang, J. Liu, R. Zhang, What are hot and what are not in an urban landscape: quantifying and explaining the land surface temperature pattern in Beijing, China, *Landsc. Ecol.* 30 (2) (2014) 357–373, <https://doi.org/10.1007/s10980-014-0128-6>.

- [211] P.J. Hardin, R.R. Jensen, The effect of urban leaf area on summertime urban surface kinetic temperatures: a Terre Haute case study, *Urban For. Urban Green.* 6 (2) (2007) 63–72, <https://doi.org/10.1016/j.ufug.2007.01.005>.
- [212] W. Zhou, G. Huang, M.L. Cadenasso, Does spatial configuration matter? Understanding the effects of land cover pattern on land surface temperature in urban landscapes, *Landscl. Urban Plann.* 102 (1) (2011) 54–63, <https://doi.org/10.1016/j.landurbplan.2011.03.009>.
- [213] A. Chen, L. Yao, R. Sun, L. Chen, How many metrics are required to identify the effects of the landscape pattern on land surface temperature? *Ecol. Indicat.* 45 (2014) 424–433, <https://doi.org/10.1016/j.ecolind.2014.05.002>.
- [214] X. Li, W. Zhou, Z. Ouyang, W. Xu, H. Zheng, Spatial pattern of greenspace affects land surface temperature: evidence from the heavily urbanized Beijing metropolitan area, China, *Landscl. Ecol.* 27 (6) (2012) 887–898, <https://doi.org/10.1007/s10980-012-9731-6>.
- [215] M. Jagamohan, S. Knapp, C.M. Buchmann, N. Schwarz, The bigger, the better? The influence of urban green space design on cooling effects for residential areas, *J. Environ. Qual.* 45 (1) (2016) 134–145, <https://doi.org/10.2134/jeq2015.01.0062>.
- [216] G.E. Kyriakidis, M. Santamouris, Using reflective pavements to mitigate urban heat island in warm climates - results from a large scale urban mitigation project, *Urban Clim.* 24 (2018) 326–339, <https://doi.org/10.1016/j.uclim.2017.02.002>.
- [217] M. Taleghani, U. Berardi, The effect of pavement characteristics on pedestrians' thermal comfort in Toronto, *Urban Clim.* 24 (2018) 449–459, <https://doi.org/10.1016/j.uclim.2017.05.007>.
- [218] Y. Wang, U. Berardi, H. Akbari, Comparing the effects of urban heat island mitigation strategies for Toronto, Canada, *Energy Build.* 114 (2016) 2–19, <https://doi.org/10.1016/j.enbuild.2015.06.046>.
- [219] Y. Qin, Urban canyon albedo and its implication on the use of reflective cool pavements, *Energy Build.* 96 (2015) 86–94, <https://doi.org/10.1016/j.enbuild.2015.03.005>.
- [220] Y. Qin, A review on the development of cool pavements to mitigate urban heat island effect, *Renew. Sustain. Energy Rev.* 52 (2015) 445–459, <https://doi.org/10.1016/j.rser.2015.07.177>.
- [221] H. Takebayashi, M. Moriyama, Study on the urban heat island mitigation effect achieved by converting to grass-covered parking, *Sol. Energy* 83 (8) (2009) 1211–1223, <https://doi.org/10.1016/j.solener.2009.01.019>.
- [222] A. Ferrari, A. Kibilay, D. Derome, J. Carmeliet, The use of permeable and reflective pavements as a potential strategy for urban heat island mitigation, *Urban Clim.* 31 (2020), <https://doi.org/10.1016/j.uclim.2019.100534>.
- [223] A. Kibilay, A. Ferrari, D. Derome, J. Carmeliet, Smart wetting of permeable pavements as an evaporative-cooling measure for improving the urban climate during heat waves, *J. Build. Phys.* 45 (1) (2020) 36–66, <https://doi.org/10.1177/1744259120968586>.
- [224] T. Nakayama, T. Fujita, Cooling effect of water-holding pavements made of new materials on water and heat budgets in urban areas, *Landscl. Urban Plann.* 96 (2) (2010) 57–67, <https://doi.org/10.1016/j.landurbplan.2010.02.003>.
- [225] Z. Shi, J.A. Fonseca, A. Schlueter, A review of simulation-based urban form generation and optimization for energy-driven urban design, *Build. Environ.* 121 (2017) 119–129, <https://doi.org/10.1016/j.buildenv.2017.05.006>.
- [226] J. Zhang, P. Cui, H. Song, Impact of urban morphology on outdoor air temperature and microclimate optimization strategy base on Pareto optimality in Northeast China, *Build. Environ.* 180 (2020), <https://doi.org/10.1016/j.buildenv.2020.107035>.
- [227] X. Shi, Z. Tian, W. Chen, B. Si, X. Jin, A review on building energy efficient design optimization from the perspective of architects, *Renew. Sustain. Energy Rev.* 65 (2016) 872–884, <https://doi.org/10.1016/j.rser.2016.07.050>.
- [228] Z. Tian, X. Zhang, X. Jin, X. Zhou, B. Si, X. Shi, Towards adoption of building energy simulation and optimization for passive building design: a survey and a review, *Energy Build.* 158 (2018) 1306–1316, <https://doi.org/10.1016/j.enbuild.2017.11.022>.
- [229] Z. Yu, S. Chen, N.H. Wong, M. Ignatius, J. Deng, Y. He, D.J.C. Hii, Dependence between urban morphology and outdoor air temperature: a tropical campus study using random forests algorithm, *Sustain. Cities Soc.* 61 (2020), <https://doi.org/10.1016/j.scs.2020.102200>.
- [230] S. Chen, W. Zhang, N.H. Wong, M. Ignatius, Combining CityGML files and data-driven models for microclimate simulations in a tropical city, *Build. Environ.* 185 (2020), <https://doi.org/10.1016/j.buildenv.2020.107314>.
- [231] J. Yang, J. Ren, D. Sun, X. Xiao, J. Xia, C. Jin, X. Li, Understanding land surface temperature impact factors based on local climate zones, *Sustain. Cities Soc.* 69 (2021), <https://doi.org/10.1016/j.scs.2021.102818>.
- [232] D. Taleb, B. Abu-Hijleh, Urban heat islands: potential effect of organic and structured urban configurations on temperature variations in Dubai, UAE, *Renew. Energy* 50 (2013) 747–762, <https://doi.org/10.1016/j.renene.2012.07.030>.
- [233] Z. Tian, X. Zhang, S. Wei, S. Du, X. Shi, A review of data-driven building performance analysis and design on big on-site building performance data, *J. Build. Eng.* 41 (2021), <https://doi.org/10.1016/j.jobe.2021.102706>.